Key Experiments

10 June 2015

HELMHOLTZ
ASSOCIATION
Helmholtz Institute Jena

GSI

Plan of lectures

- 1 15.04.2015 Preliminary Discussion / Introduction

- 2 22.04.2015 Experiments (discovery of the positron, formation of antihydrogen, ...)
- 3 29.04.2015 Experiments (Lamb shift, hyperfine structure, quasimolecules and MO spectra)
- 4 06.05.2015 Theory (from Schrödinger to Dirac equation, solutions with negative energy)
- 5 13.05.2015 Theory (bound-state solutions of Dirac equation, quantum numbers)
- 6 20.05.2015 Theory (bound-state Dirac wavefunctions, QED corrections)

- 7 27.05.2015 Experiment (photoionization, radiative recombination, ATI, HHG...)
- 8 03.06.2015 Theory (description of the light-matter interaction)
- 9 10.06.2015 Experiment (Kamiokande, cancer therapy, ….)

- 10 17.06.2015 Experiment (Auger decay, dielectronic recombination, double ionization)
- 11 24.06.2015 Theory (interelectronic interactions, extension of Dirac (and Schrödinger) theory for the description of many-electron systems, approximate methods)

- 12 01.07.2015 Theory (atomic-physics tests of the Standard Model, search for a new physics)
- 13 08.07.2015 Experiment (Atomic physics PNC experiments (Cs,...), heavy ion PV research)

Content of this Lecture

- Kamiokande experiment
  - Neutrino oscillations

- Hadron therapy

Beta decay: Neutron is converted to proton

Shell model for neutrons and protons

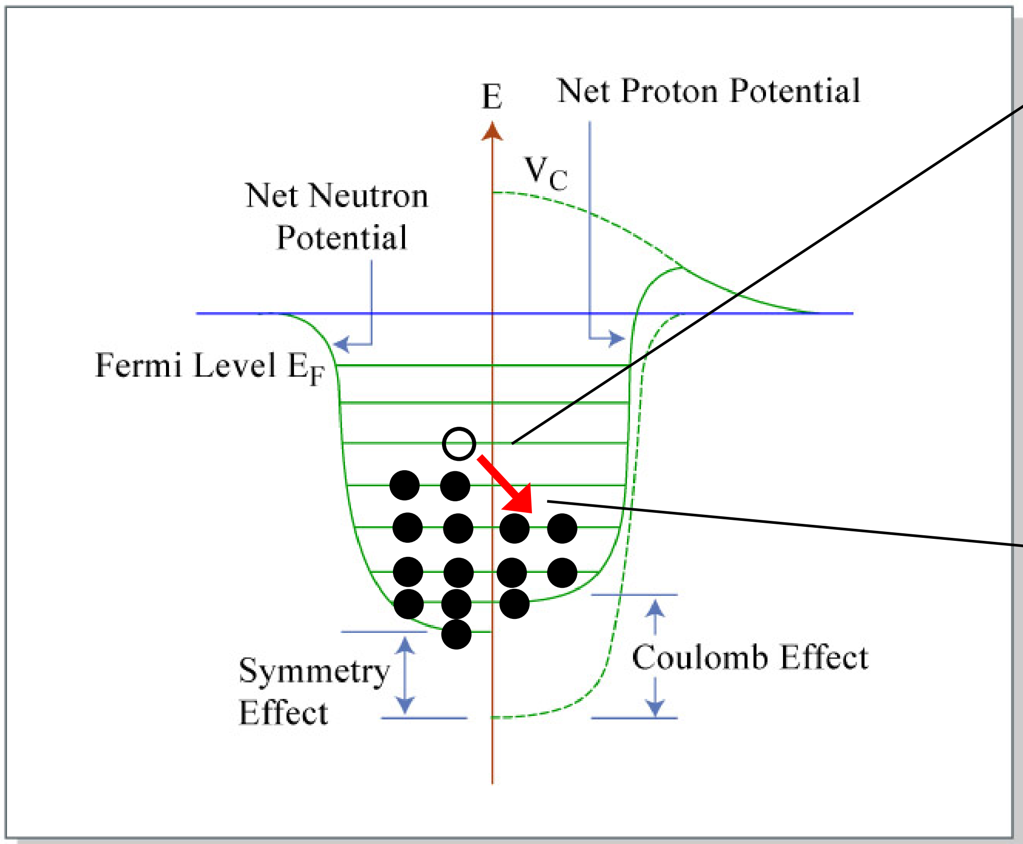

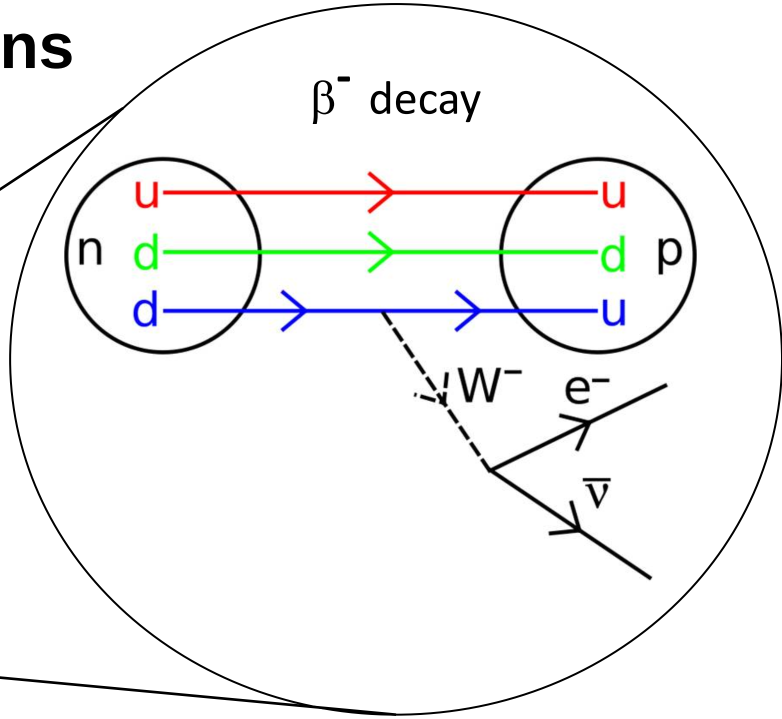

Beta decay results in a higher binding energy of the nucleus.

β^+ decay (p → n) also possible.

Electron/Positron and Neutrino are emitted.

Reminder: Standard Model

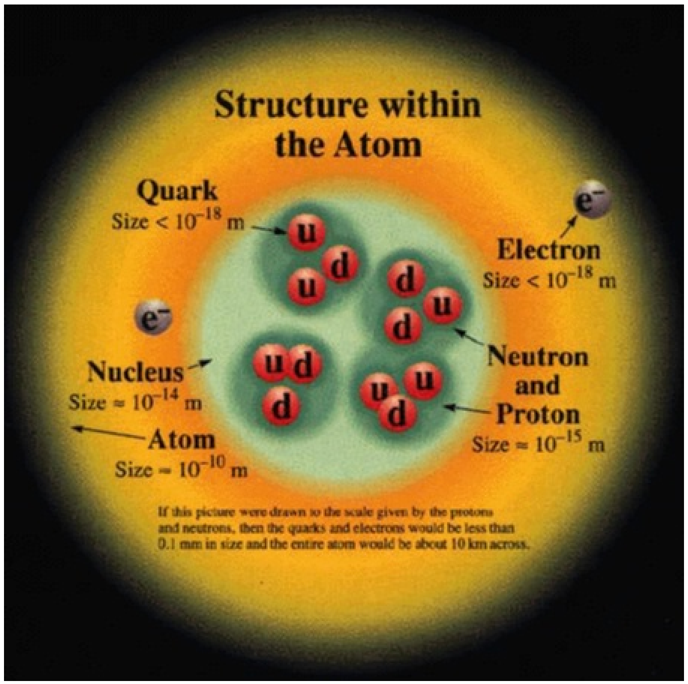

BOSONS

force carriers
spin = 0, 1, 2,...

Unified Electroweak spin = 1	Mass GeV/c²	Electric charge
γ photon	0	0
W^-	80.22	–1
W^+	80.22	+1
Z^0	91.187	0

Strong or color spin = 1	Mass GeV/c²	Electric charge
g gluon	0	0

FERMIONS

matter constituents
spin = 1/2, 3/2, 5/2,...

Leptons spin = 1/2

Flavor	Mass GeV/c²	Electric charge
ν_e electron neutrino	$< 7 \times 10^{-9}$	0
e electron	0.000511	–1
ν_μ muon neutrino	< 0.0003	0
μ muon	0.106	–1
ν_τ tau neutrino	< 0.03	0
τ tau	1.7771	–1

Quarks spin = 1/2

Flavor	Approx. Mass GeV/c²	Electric charge
u up	0.005	2/3
d down	0.01	–1/3
c charm	1.5	2/3
s strange	0.2	–1/3
t top (initial evidence)	170	2/3
b bottom	4.7	–1/3

Lepton type (number) is conserved

Leptons are divided into three **lepton families**: the electron and its neutrino, the muon and its neutrino, and the tau and its neutrino.

$$p \rightarrow n + e^{+} + \nu \qquad\qquad n \rightarrow p + e^{-} + \bar{\nu}$$

Electron number	**+1:** $e^{-};\nu_e$	**-1:** $e^{+};\bar{\nu}_e$
Myon number	**+1:** $\mu^{-};\nu_\mu$	**-1:** $\mu^{+};\bar{\nu}_\mu$
Tau number	**+1:** $\tau^{-};\nu_\tau$	**-1:** $\tau^{+};\bar{\nu}_\tau$

	muon		muon neutrino		electron		e^- antineutrino
equation:	μ	$\rightarrow$	ν_μ	$+$	e^-	$+$	$\bar{\nu}_e$
electron number:	0	=	0	+	1	+	-1
muon number:	1	=	1	+	0	+	0
tau number:	0	=	0	+	0	+	0

Neutrinos: Many questions are still open!

Type	Elementary particle
Statistics	Fermionic
Generations (Flavour)	First, second and third
Interactions	Weak interaction and gravitation
Antiparticle	Antineutrinos are possibly identical to the neutrino (see *Majorana fermion*).
Discovery	ν_e: Clyde Cowan, Frederick Reines (1956) ν_μ: Leon Lederman, Melvin Schwartz and Jack Steinberger (1962) ν_τ: DONUT collaboration (2000)
Types	3 – electron neutrino, muon neutrino and tau neutrino
Mass	Small, but non-zero. See the *mass* section.
Electric Charge	0
Spin	$^1/_2$

http://en.wikipedia.org/wiki/Neutrino

Beta Decay: What about the neutrino properties?

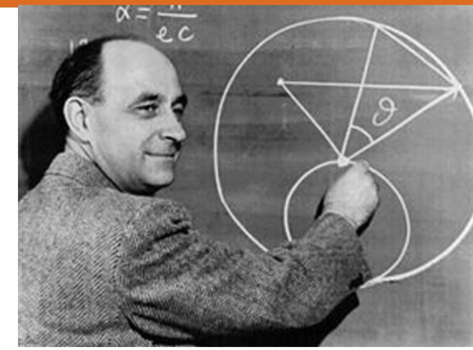

Enrico Fermi suggested in his classical paper on beta decay to measure the neutrino mass using beta decay. The electron energy is measured at the end point part of the electron energy spectrum. The experiment is done with tritium decay where a neutron in the tritium nucleus is decayed by the process:

$$^{3}H \rightarrow {}^{3}He + e^{-} + \overline{\nu}$$

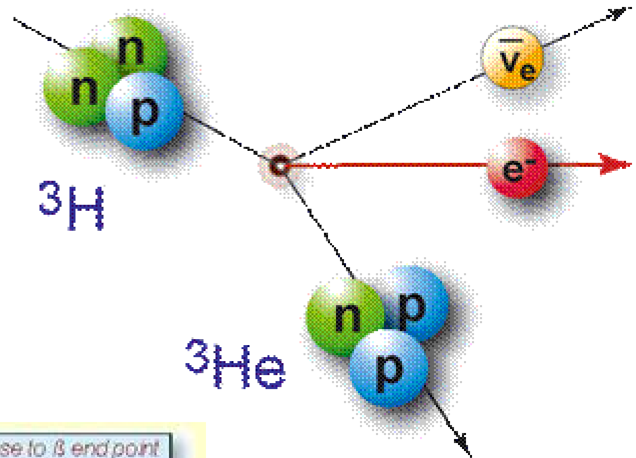

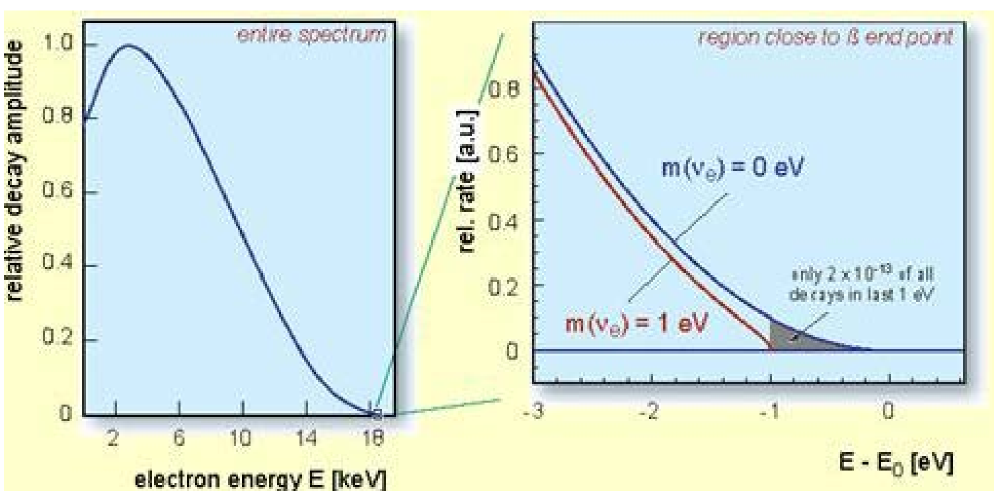

The entire spectrum of the electron kinetic energy in the tritium beta decay is shown in a. The end point is shown enlarged in b. For neutrino to have mass the kinetic energy of the electron should be slightly smaller then the energy released by the beta decay as shown by the red line. Actual result from measuring the electron kinetic energy shows no indication of massive neutrinos. (Image by the Katrin collaboration)

Search for Neutrino mass

Two kind of experiments:

- Direct electron neutrino-mass experiments

KATRIN

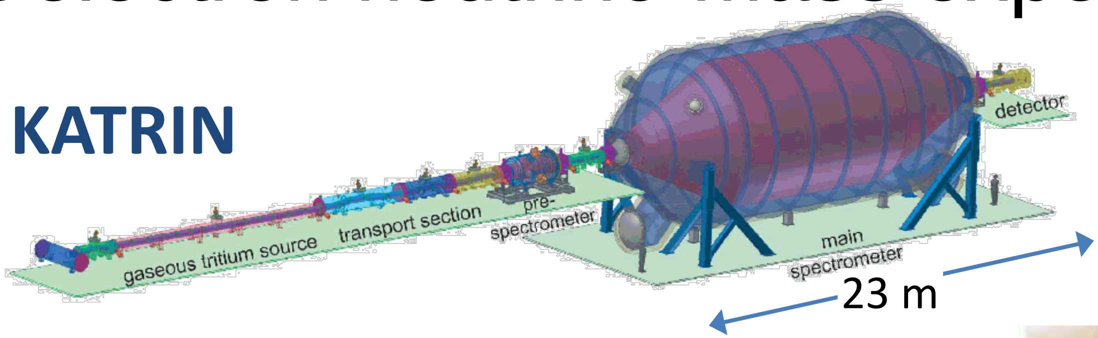

- Neutrino oscillation experiments

SUPER-KAMIOKANDE

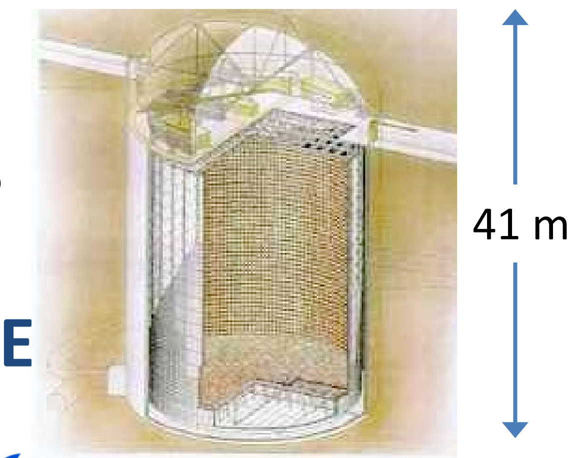

HELMHOLTZ ASSOCIATION
Helmholtz Institute Jena
GSI

Karlsruhe Tritium Neutrino Experiment (KATRIN)

The Tritium Neutrino Experiment (KATRIN) is aiming on a direct determination of the electron neutrino mass. Currently it is getting installed at KIT (Karlsruhe).

MAC-E-Filter *(Magnetic Adiabatic Collimation combined with an Electrostatic Filter)* are used to determine electron energies of the tritium beta decay.

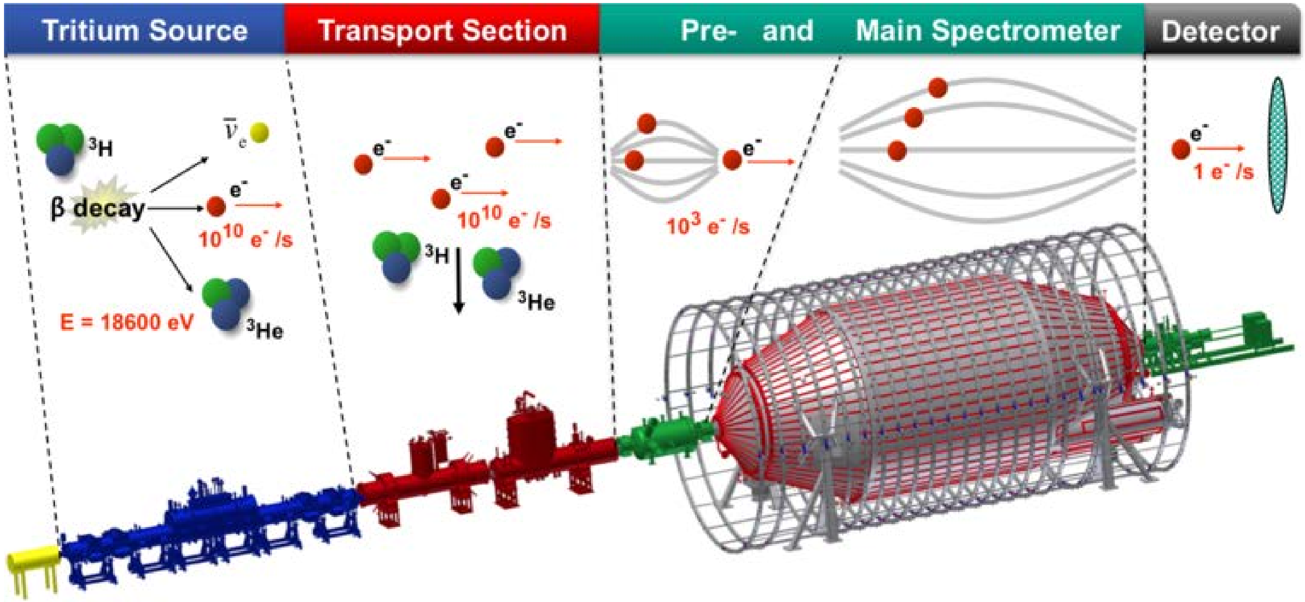

Tritium decays, releasing an electron and an anti-electron-neutrino. While the neutrino escapes undetected, the electron starts its journey to the detector.

Electrons are guided towards the spectrometer by magnetic fields. Tritium has to be pumped out to provide tritium free spectrometers.

The electron energy is analyzed by applying an electrostatic retarding potential. Electrons are only transmitted if their kinetic energy is sufficiently high.

At the end of their journey, the electrons are counted at the detector. Their rate varies with the spectrometer potential and hence gives an integrated β-spectrum.

Aiming for the endpoint of the continuous electron distribution with 1 eV precision.

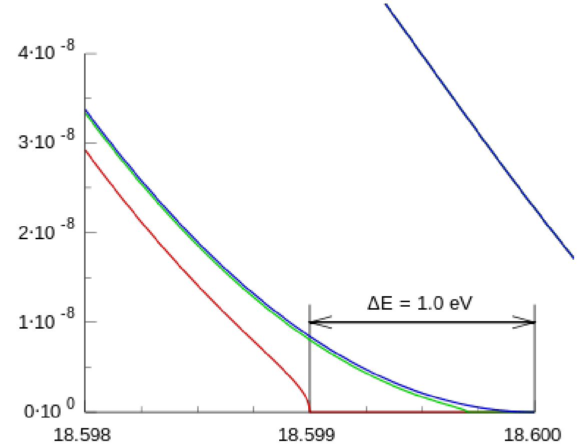

HELMHOLTZ | ASSOCIATION

Helmholtz Institute Jena

GSI

The Super-Kamiokande Experiment

Investigation of the atmospheric neutrino problem. Are there neutrino oscillations?

Electrons Electron neutrino	Myon Myon neutrino	Tau Tau neutrino
m_e 511 keV/c²	m_μ 106 MeV/c²	m_τ 1777 MeV/c²

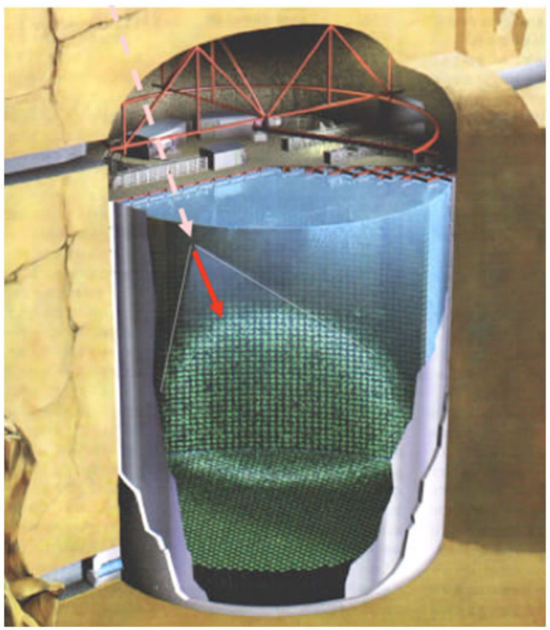

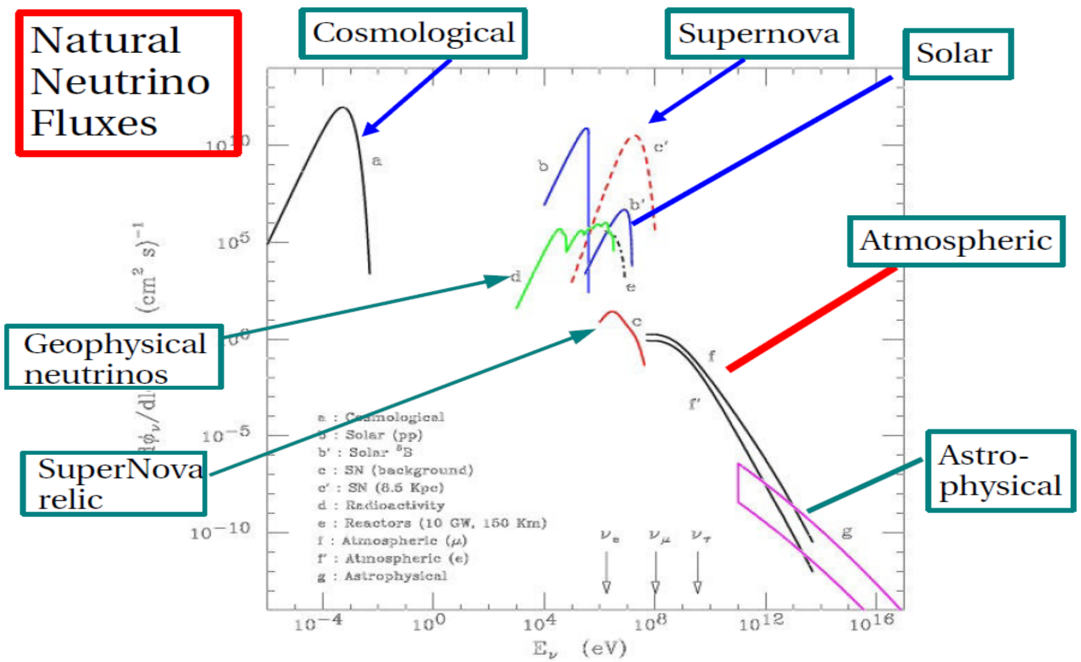

Atmospheric Neutrino Production

After being generated in the upper atmosphere the neutrinos may interact with matter resulting in the production of electrons/positrons and neutrinos from lower generations.

muon neutrinos

$$\nu_\mu + n \rightarrow \mu^- + p$$

$$\downarrow$$

$$\mu^- \rightarrow e^- + \nu_e + \nu_\mu$$

$$\nu_\mu + p \rightarrow \mu^+ + n$$

$$\downarrow$$

$$\mu^+ \rightarrow e^+ + \nu_e + \nu_\mu$$

electron neutrinos

$$\nu_e + n \rightarrow e^- + p$$

$$\nu_e + p \rightarrow e^+ + n$$

Typical cross section: $\sigma \approx 10^{-38}\ \text{cm}^2$

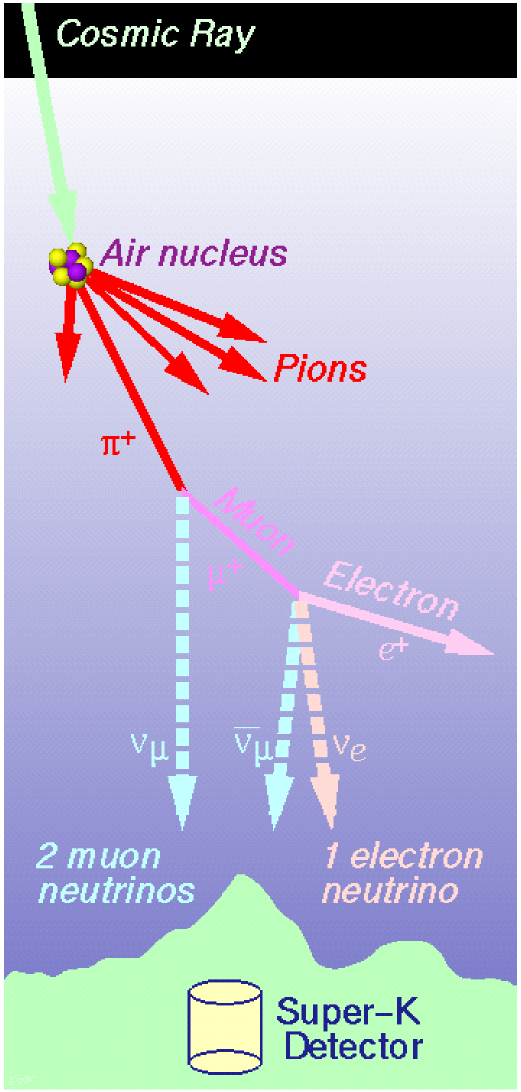

Identification of the Neutrino Types

Primary cosmic radiation:
~95% protons, ~4.5% α-particles. They produce mesons (Pions, Kaons).

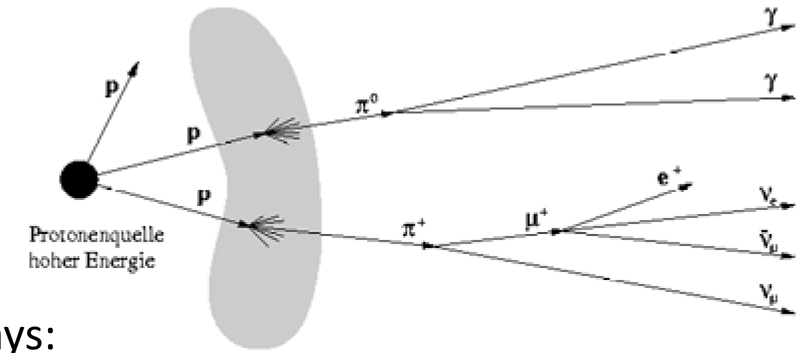

Neutrinos from the atmosphere:
E > 100 MeV

Typical meson decays:

$$\pi^- \rightarrow \mu^- + \overline{\nu_\mu}$$
$$\mu^- \rightarrow e^- + \overline{\nu_e} + \nu_\mu$$

$$\pi^+ \rightarrow \mu^+ + \nu_\mu$$
$$\mu^+ \rightarrow e^+ + \nu_e + \overline{\nu_\mu}$$

Prediction:
Ratio (myon neutrino kind of events / (electron neutrino kind of events) ≈ 2

Observation:
Ratio (myon neutrino kind of events / (electron neutrino kind of events) ≈ 1

Neutrino Oscillations: Basic Considerations

Assumption: Neutrinos have different, finite masses

Eigenstates of the interaction

$$(\nu_e, \nu_\mu, \nu_\tau)$$

Mass Eigenstates

$$(\nu_1, \nu_2, \nu_3)$$

Example: Oscillation between two different neutrinos

Eigenstates of the interaction

$$(\nu_e, \nu_\mu)$$

Mass Eigenstates

$$(\nu_1, \nu_2)$$

$$|\upsilon_\mu\rangle = \cos\theta\,|\upsilon_1\rangle + \sin\theta\,|\upsilon_2\rangle$$

$$|\upsilon_\mu(t)\rangle = \cos\theta|\upsilon_1\rangle e^{-i/\hbar\, E_1 t} + \sin\theta|\upsilon_2\rangle e^{-i/\hbar\, E_2 t}$$

$$E_j = \sqrt{p_j^2 c^2 + m_j^2 c^4} \qquad j = 1,2$$

Neutrino Oscillations: Basic Considerations

Example: Oscillation between two different neutrinos

Eigenstates of the interaction

$$(\nu_e, \nu_\mu)$$

Mass Eigenstates

$$(\nu_1, \nu_2)$$

$$|\upsilon_\mu\rangle = \cos\theta\,|\upsilon_1\rangle + \sin\theta\,|\upsilon_2\rangle$$

$$|\upsilon_\mu(t)\rangle = \cos\theta|\upsilon_1\rangle e^{-i/\hbar\, E_1 t} + \sin\theta|\upsilon_2\rangle e^{-i/\hbar\, E_2 t}$$

$$E_j = \sqrt{p_j{}^2 c^2 + m_j{}^2 c^4} \qquad j = 1,2$$

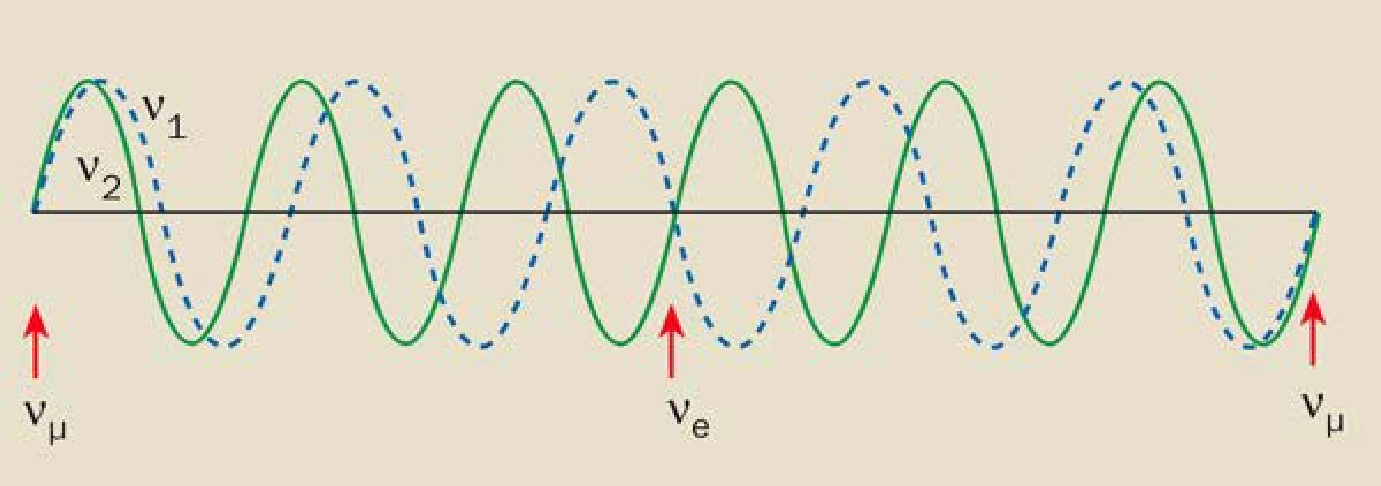

Neutrino Oscillations: Basic Considerations

Assumption: Neutrinos have different, finite masses

Eigenstates of the interaction

$$(\nu_e, \nu_\mu, \nu_\tau)$$

Mass Eigenstates

$$(\nu_1, \nu_2, \nu_3)$$

Example: Oscillation between two different neutrinos

Eigenstates of the interaction

$$(\nu_e, \nu_\mu)$$

Mass Eigenstates

$$(\nu_1, \nu_2)$$

$$|\upsilon_\mu\rangle = \cos\theta\,|\upsilon_1\rangle + \sin\theta\,|\upsilon_2\rangle$$

$$|\upsilon_\mu(t)\rangle = \cos\theta|\upsilon_1\rangle e^{-i/\hbar\, E_1 t} + \sin\theta|\upsilon_2\rangle e^{-i/\hbar\, E_2 t}$$

$$E_j = \sqrt{p_j^{\,2} c^2 + m_j^{\,2} c^4} \qquad j = 1,2$$

$$\left|\langle \upsilon_\mu(t)|\upsilon_\mu(t=0)\rangle\right|^2 = P(\upsilon_\mu \rightarrow \upsilon_\mu)$$

$$P = 1 - \sin^2(2\theta)\ \sin^2(1.27\,\Delta m^2 \frac{L}{E_\nu})$$

Neutrino Oscillations: Mixing Angle and Mass Difference

After a distance L = c t :

Source ← L → Detector

Probability to find the μ-Neutrino :

$$P(\upsilon_\mu) = 1 - \sin^2(2\theta)\ \sin^2(1.27\,\Delta m^2 \frac{L}{E_\nu})$$

Probability to not find the μ-Neutrino :

$$P(\upsilon_\tau) = \sin^2(2\theta)\ \sin^2(1.27\,\Delta m^2 \frac{L}{E_\nu})$$

θ mixing angle

$\Delta m^2 = |m_1^2 - m_2^2|$ Difference of the square of the masses $[(eV/c^2)^2]$

L distance from sourve [m]

E_ν Neutrino energy [MeV]

θ = ?

Δm^2 = ?

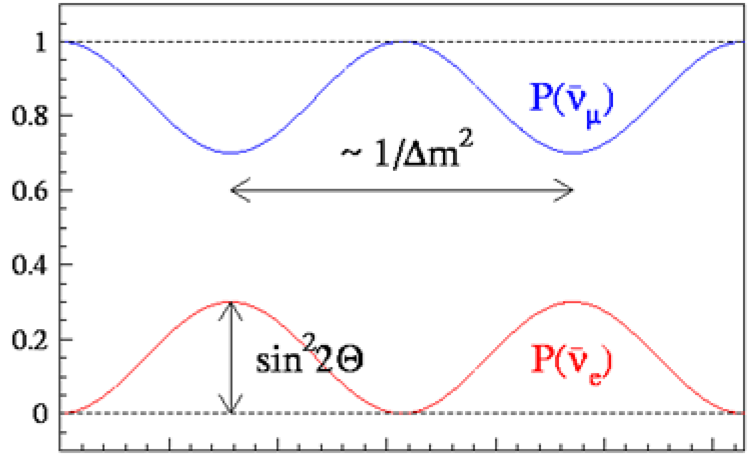

$$P(\upsilon_\mu) = 1 - \sin^2(2\theta)\ \sin^2(\pi \frac{L}{\lambda})$$

With the wavelength

$\lambda = 2{,}48\ E_\nu / \Delta m^2$

Oscillations: Atmospheric Oscillations

$$P = 1 - \sin^2(2\theta)\ \sin^2\left(\pi\frac{L}{\lambda}\right)$$

Assumption:
Maximal mixing ($\sin^2\Theta = 1$); $\Delta m^2 = 10^{-2}\ eV^2$;
Neutrino energy: 100 MeV < E < 1000 MeV

$\lambda_{MIN} \approx 250$ km $\qquad \lambda_{MAX} \approx 2500$ km

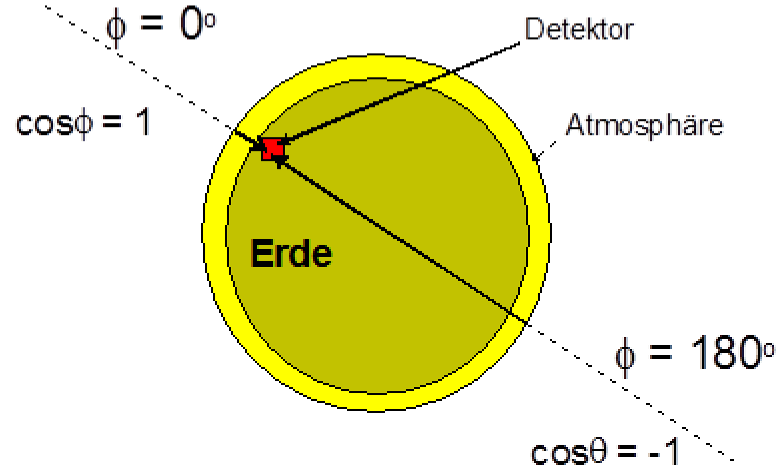

Atmosphere:	**L ≈15 km**	**<<** λ_{MIN}	⇒	**P=1**
Earth:	**L ≈13 000 km**	**>>** λ_{MAX}	⇒	**P=0.5**

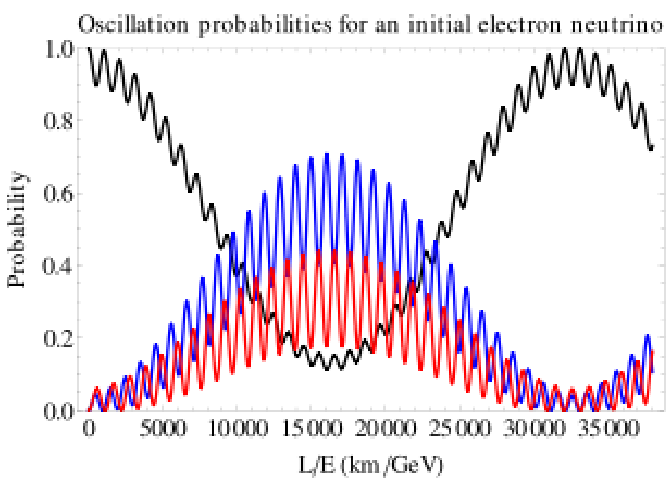

Oscillations becoming more complex with 3 neutrino types.

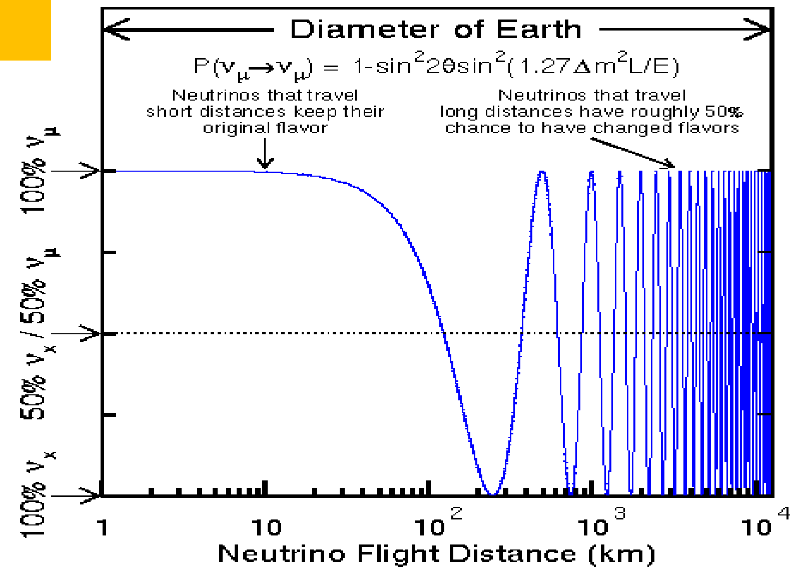

The Super-Kamionkande Detector

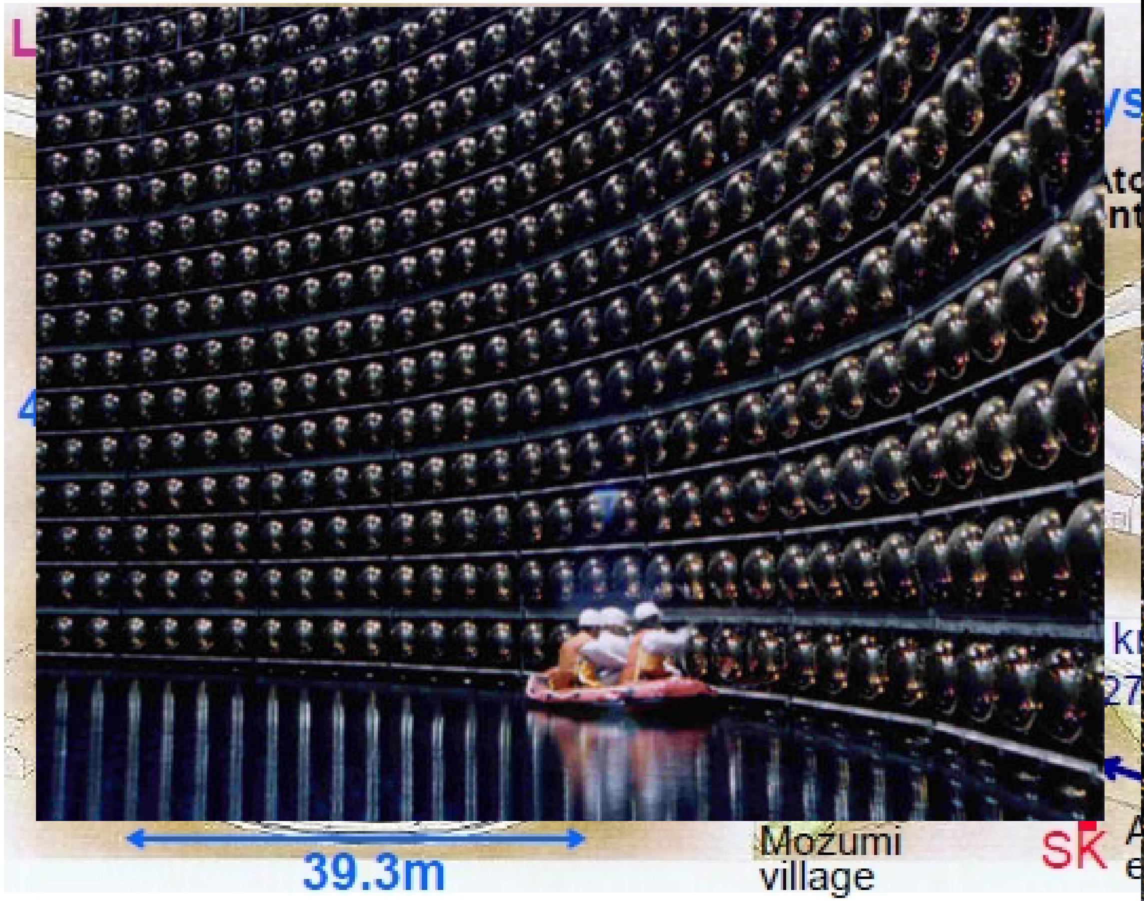

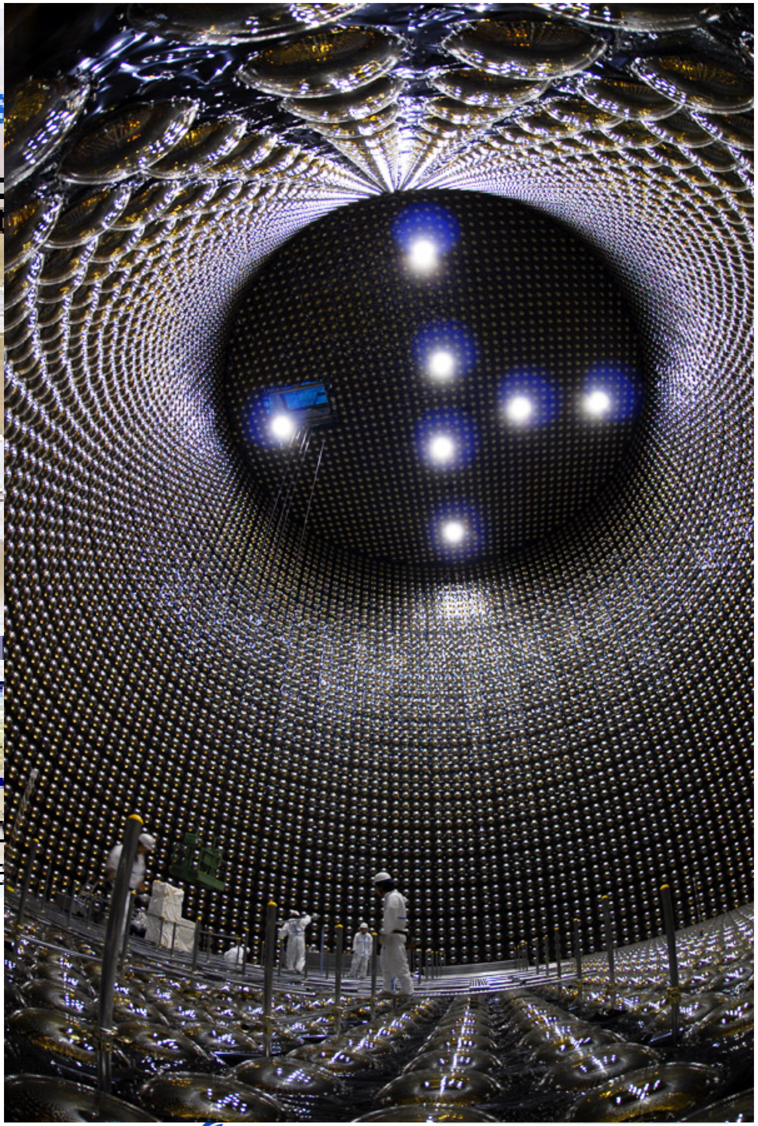

Timing: 2.5 ns
Energy resolution: 5%
Angle resolution: 2% to 7%

All materials must have extremly low radioactive activity!

Event characteristics as a function of neutrino energy

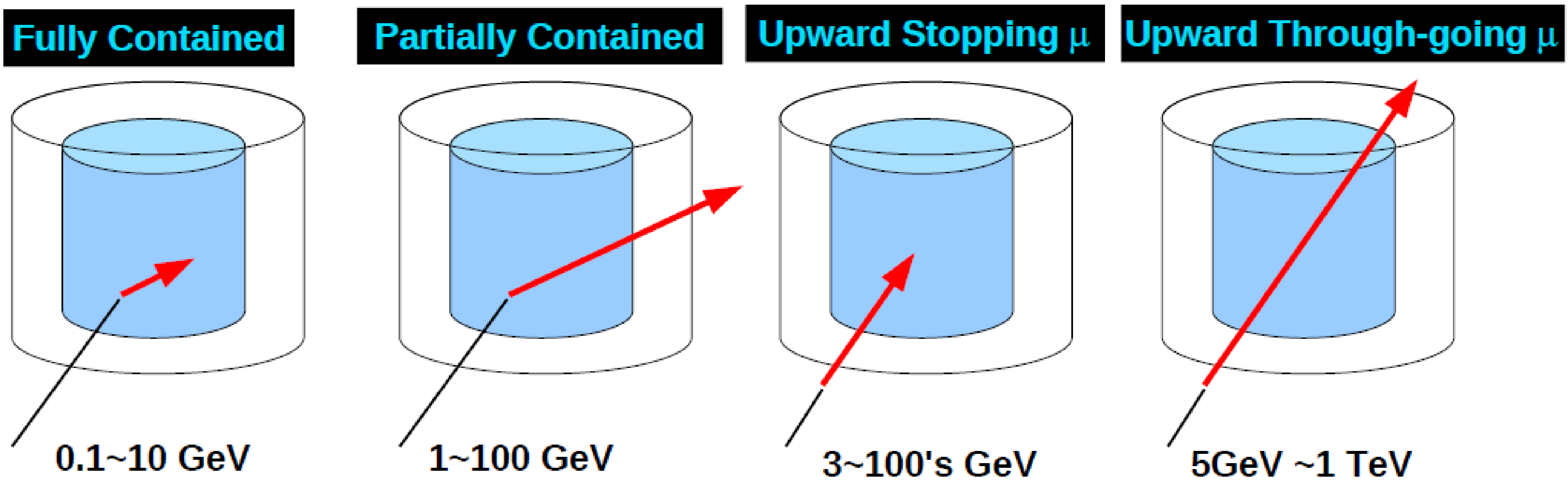

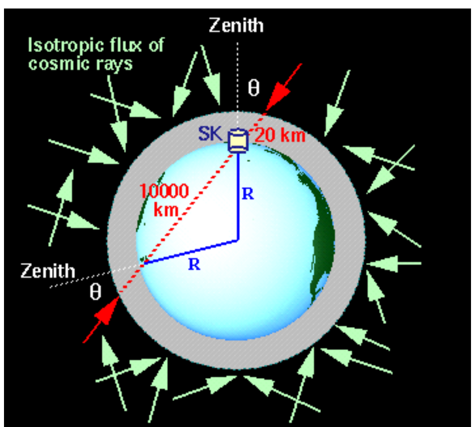

high-energy → low cross section

Neutrino-matter interaction takes place somewhere inside the earth. Only the resulting myon enters the detector vessel. Electrons cannot enter (straggling, energy loss).

Multi-GeV cosmic particles are largely unaffected by the magnetic field of the earth.
→ isotropic neutrino flux, in contrast to low-energy events

Indirect Neutrino Detection via Cherenkov Counter

Energy and momentum determination of electrons and myons

Speed of light in medium c_M : $c_M = c/n(\lambda)$

$n(\lambda)$ index of refraction

Threshold condition:
$v > c_M$

emission angle
$\cos\vartheta = c_M/V$

for water and $\beta \approx 1$:
$\theta = 42^o$:
$n(\lambda) \approx 1,4$

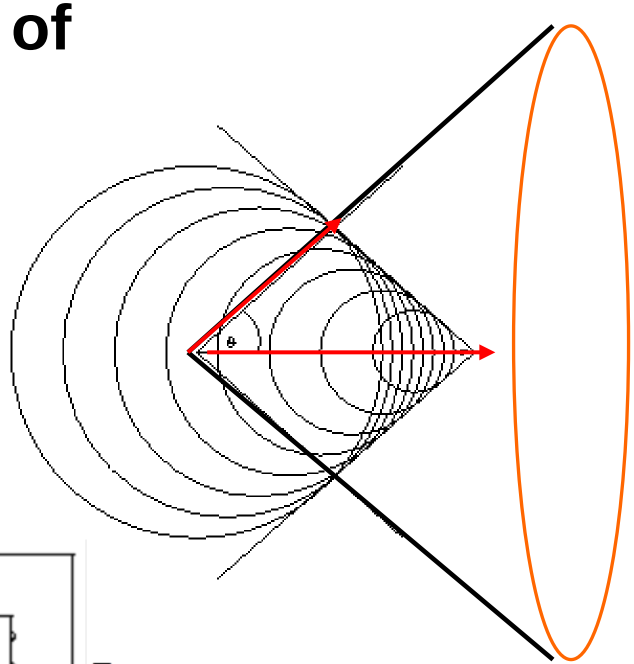

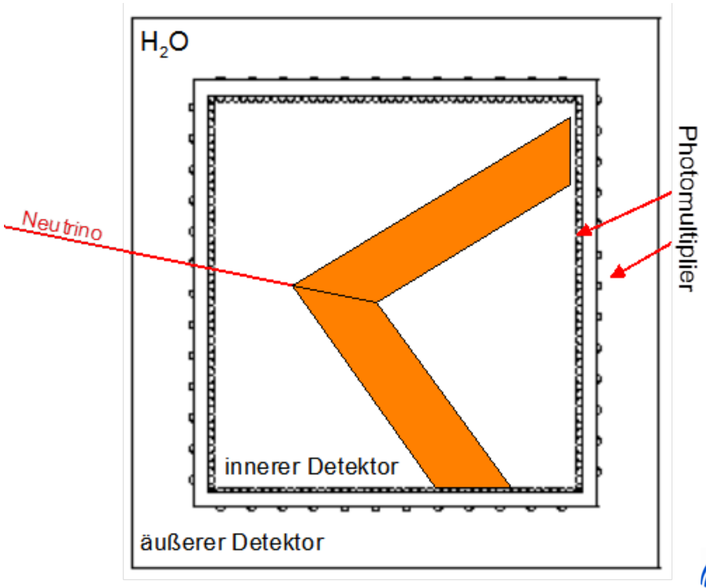

Cherenkov photons
1-2 eV

Cherenkov cone position distribution, intensity and time structure reveal details of the neutrino event

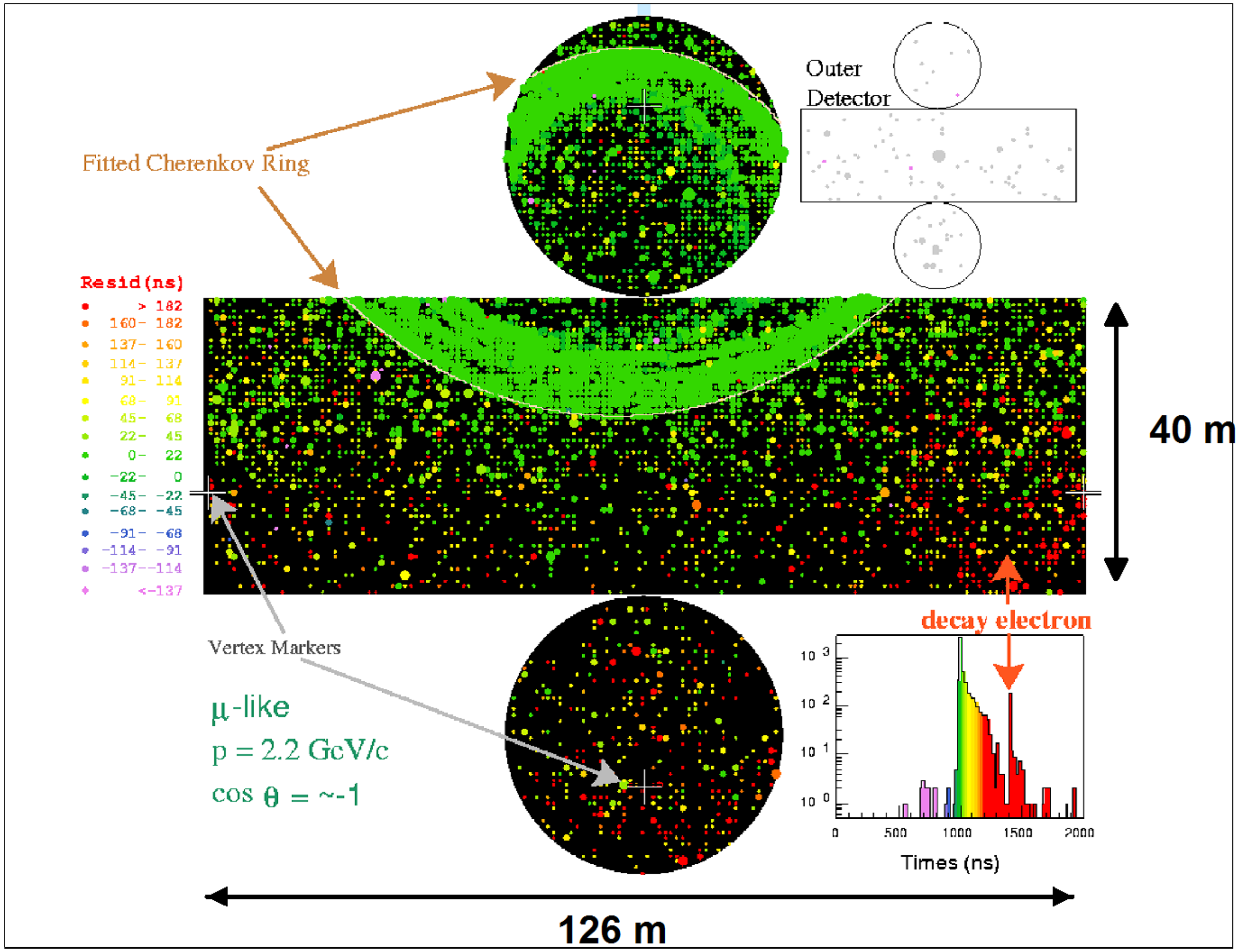

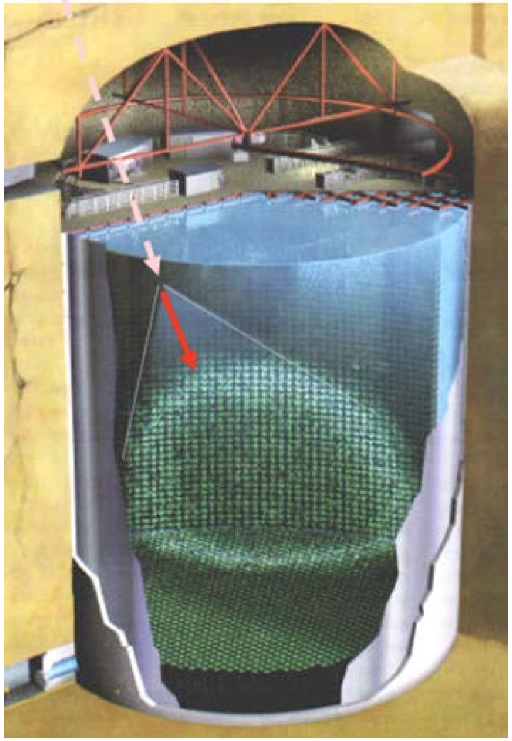

Myonic Events versus Electronic Events

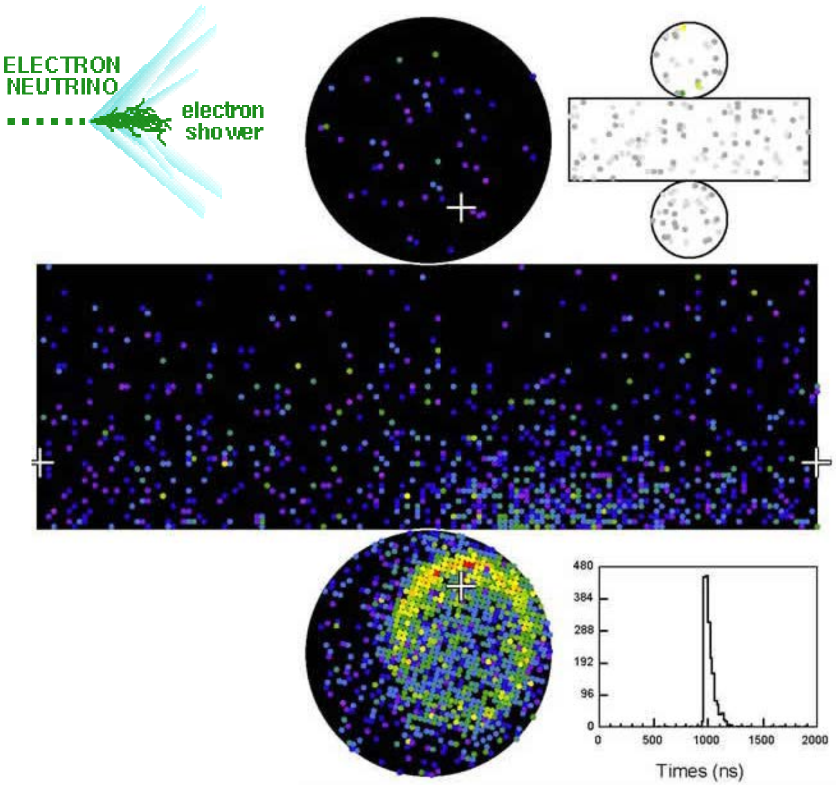

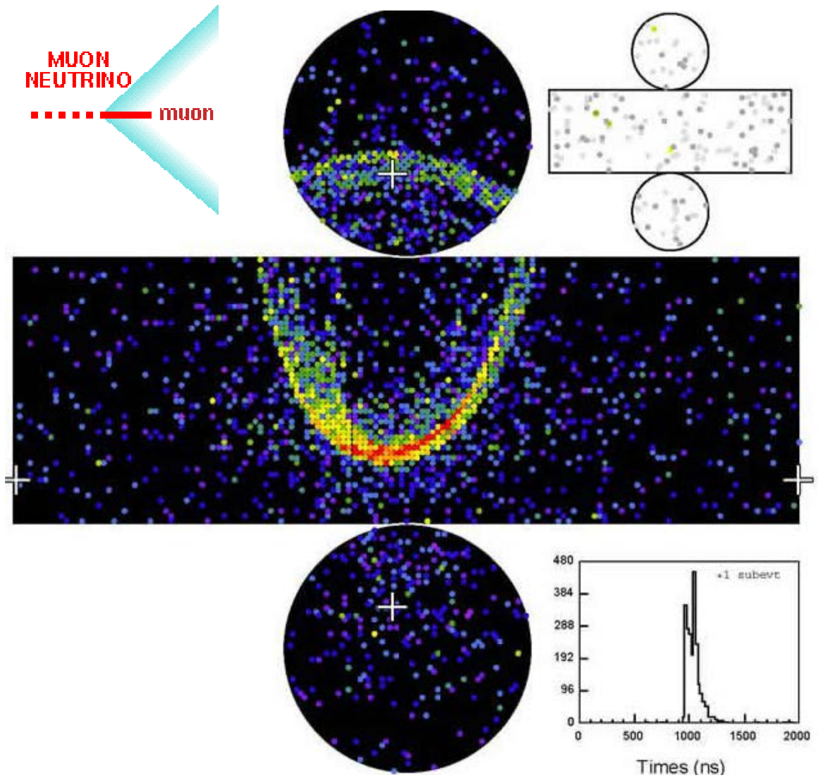

Electron:

- **more straggling**
- **electromagnetic showers**

→ ‚blurred' Cherenkov cone

Myon:

- **straight trajectory**
- **few radiative energy loss**

→ sharp Cherenkov cone

Results for atmospheric neutrinos

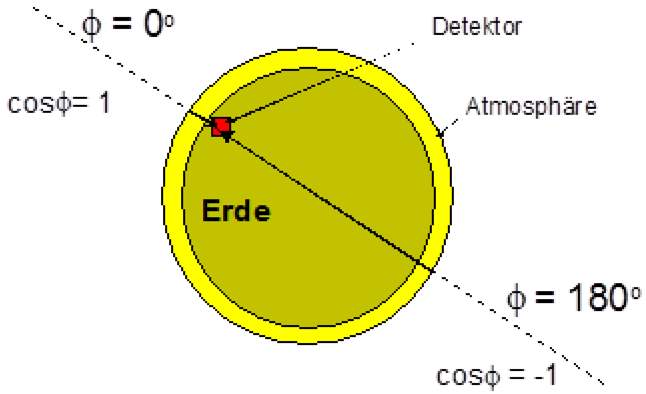

1998:

R=(μ/e)$_{measured}$ / (μ/e)$_{prediction}$

R = 0.63 ± 0.03 ± 0.05

What happend to the missing myon neutrinos?

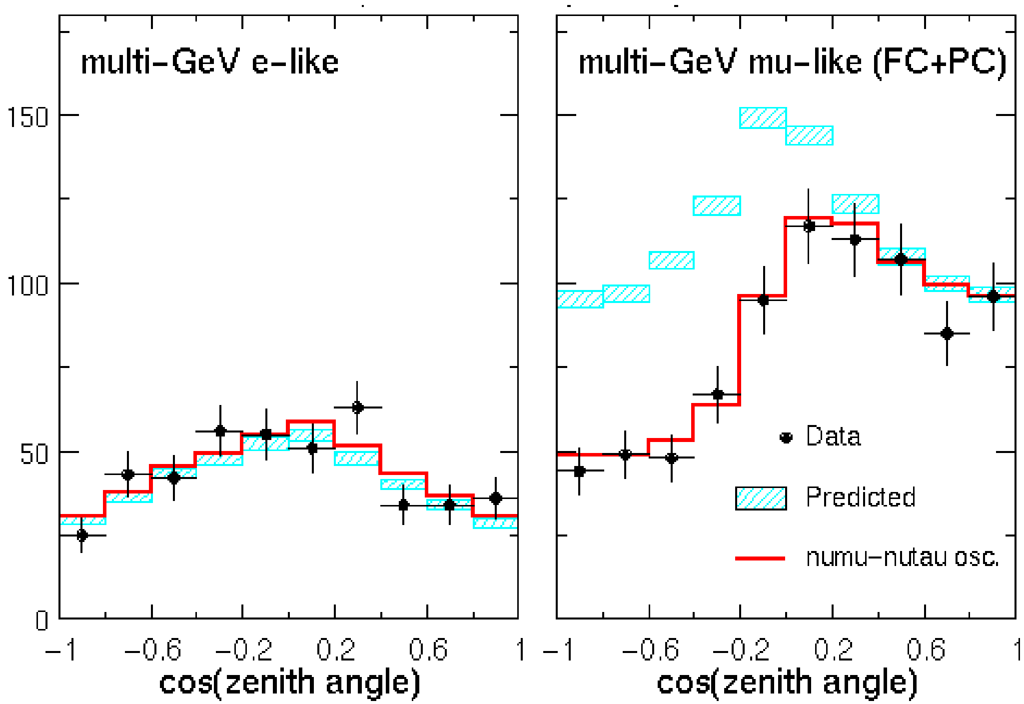

Flux of electron neutrinos agrees with expectations (no oscillation).
→ conversion to tau neutrinos is likely!

Parameter for ν_τ - ν_μ oscillations (90% confidence level)

$\sin^2\theta > 0.55$

$4\times10^{-4} < \Delta m^2 < 5 \times 10^{-2}\ eV^2$

HELMHOLTZ | ASSOCIATION
Helmholtz Institute Jena

GSI

Radiotherapy

- Also called “Radiation Therapy” (use of ionizing particles)
- Part of multi-disciplinary approach to cancer care
- Useful for 50-60% of all cancer patients
- Can be given for cure or palliation
- Mainly used for loco-regional treatment
- Benefits and side-effects are usually limited to the area(s) being treated

Charged particles for therapy

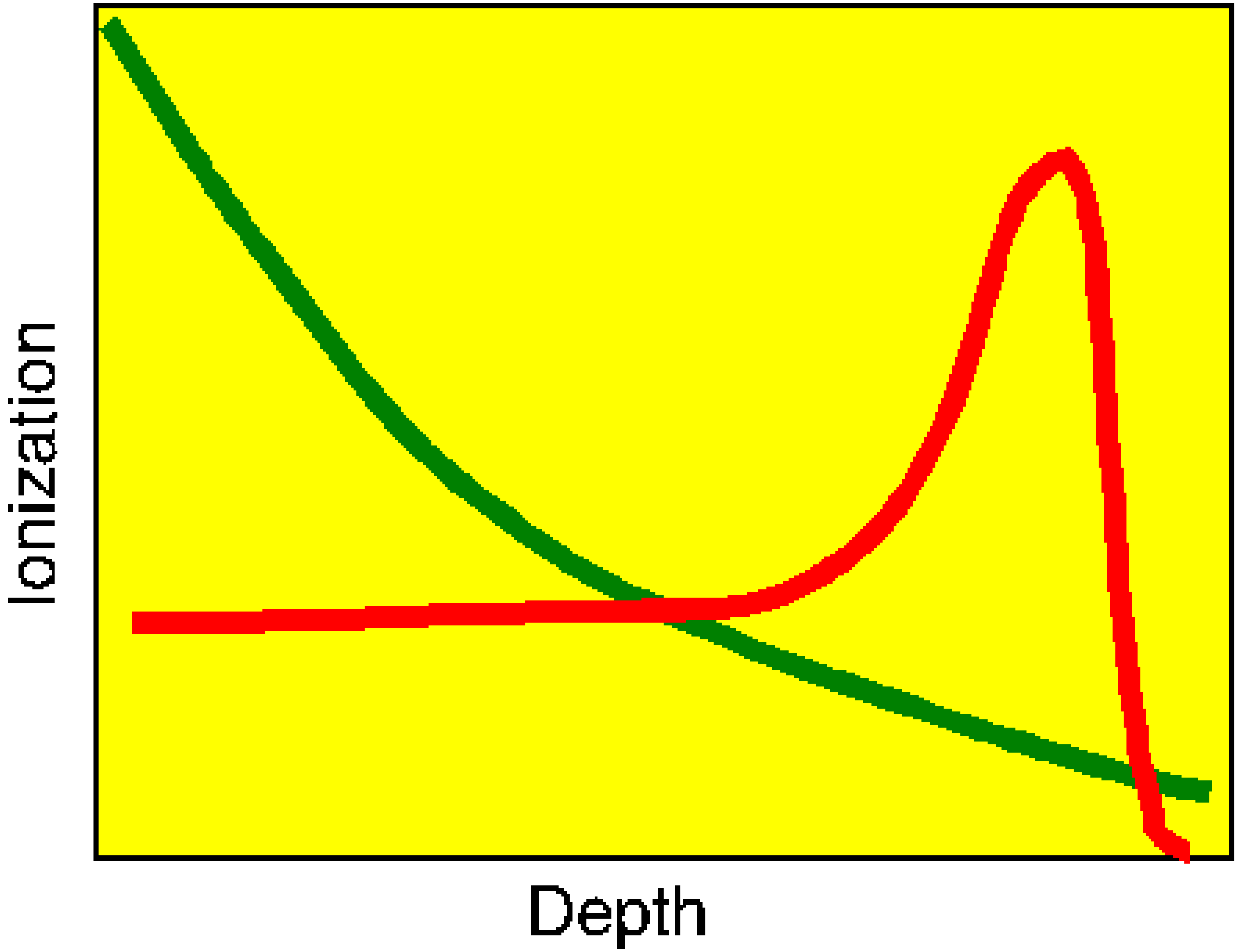

Depth dose distribution of various radiation modalities

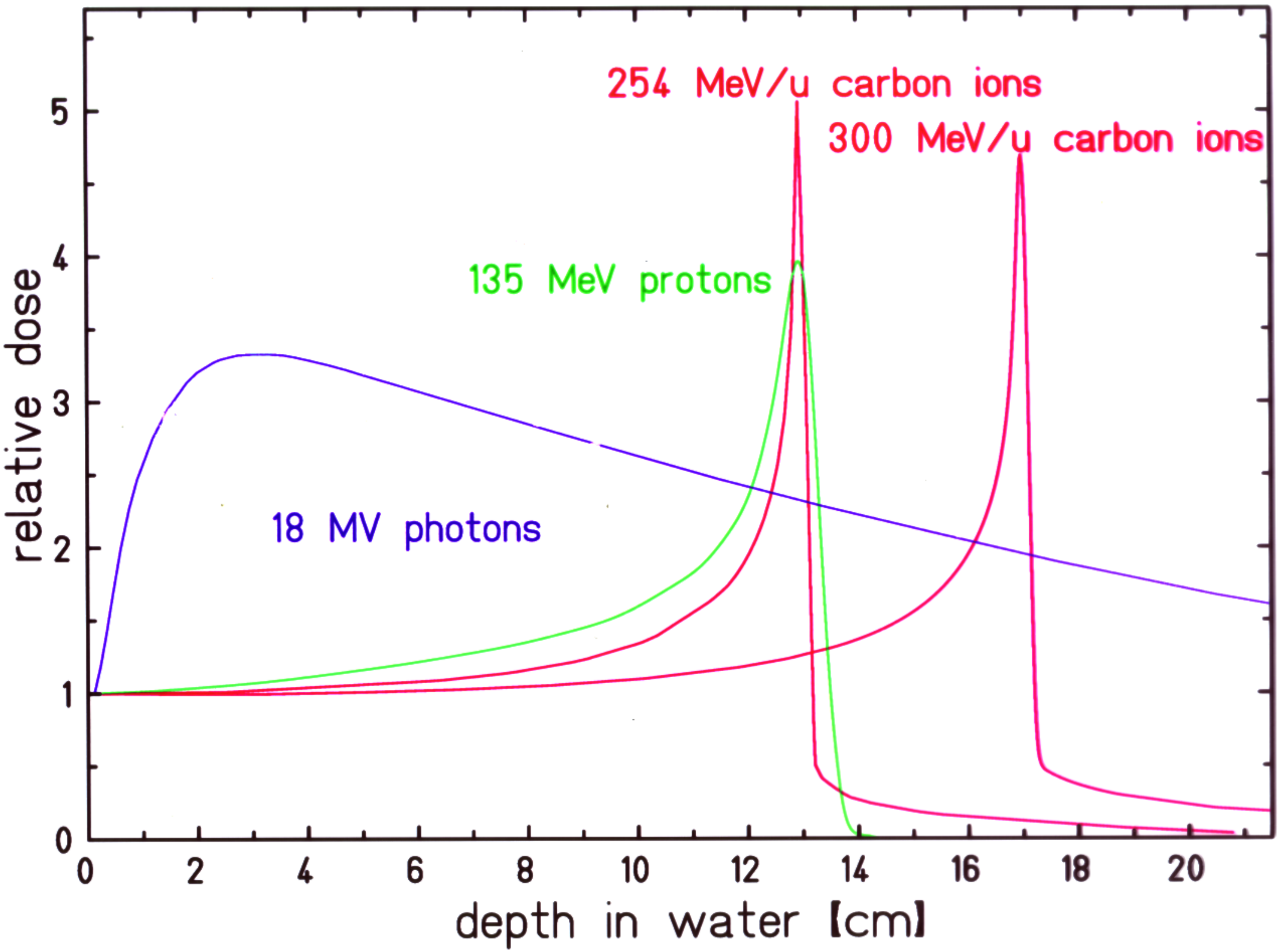

Bragg peak

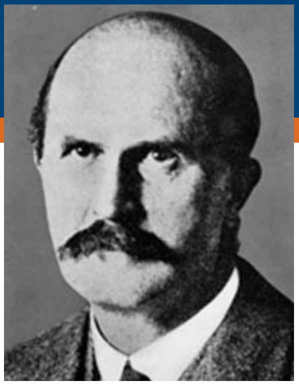

William Henry Bragg

- Since the energy loss of heavy charged particles is larger for smaller energies most of the energy is deposited by particle before stopping.
- This effect has an important applications for cancer therapy!
- A beam of heavy charged particles can be used to destroy cancer cells at given depth in the body without destroying healthy cells.

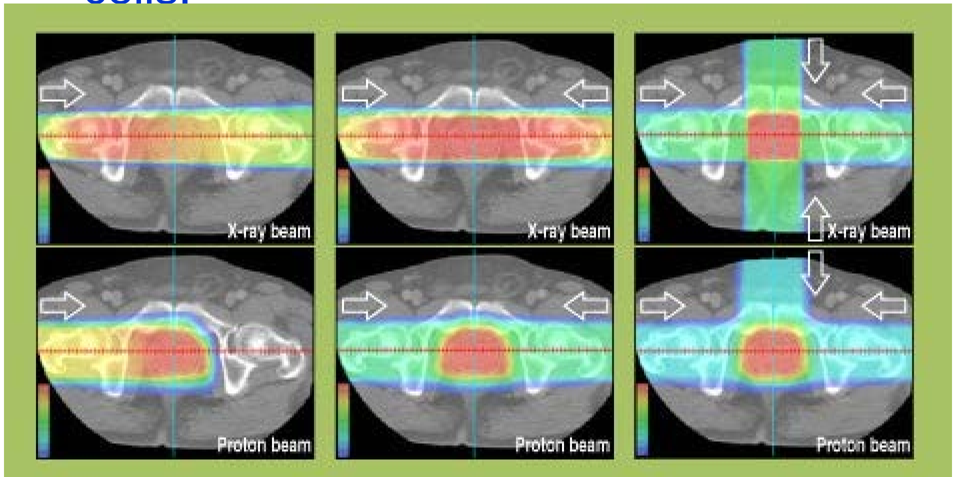

Fig. X-ray beam vs. Proton beam for prostate cancer

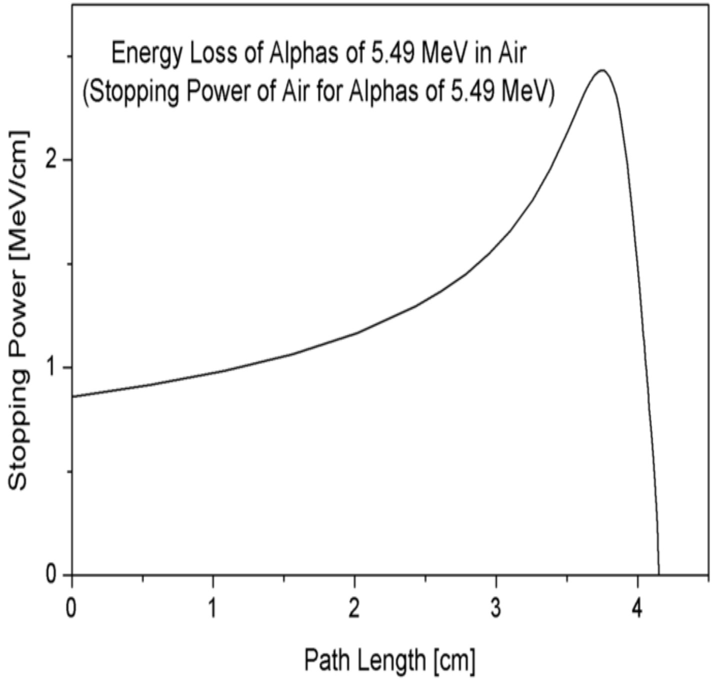

Proton and Ion Beams in Radiotherapy

- 1946 **R.R. Wilson, Radiology 47,487**
- **„… potential benefits of heavy charged**
- **particles in radiotherapy“**

- **John and Ernest Lawrence, C. Tobias**

			patients
1954 - 57	p	184-inch SC Berkeley	30
1957 - 92	^{4}He	184-inch SC Berkeley	2054
1961 – 2002	p	Harvard	9116
1969 –	p	ITEP Moscow	3785 (Dec 04)
1975 - 92	^{20}Ne	BEVALAC Berkeley	433

R.R. Wilson at Harvard mid 1940s
†2000

Clinical advantages of heavy-ion beams

- **Excellent depth-dose profile (Bragg curve)** *p, ions*
- **Increased biological effectiveness** *only ions*
- **Tumor-conform treatment** *p, ions*
  - beam scanning + energy variation
- **In-vivo range localisation** *(p), ions*
  - Positron-emitting beam fragments (PET)

HELMHOLTZ | ASSOCIATION
Helmholtz Institute Jena
GSI

Range of $^{12}C^{6+}$ Ions in Water

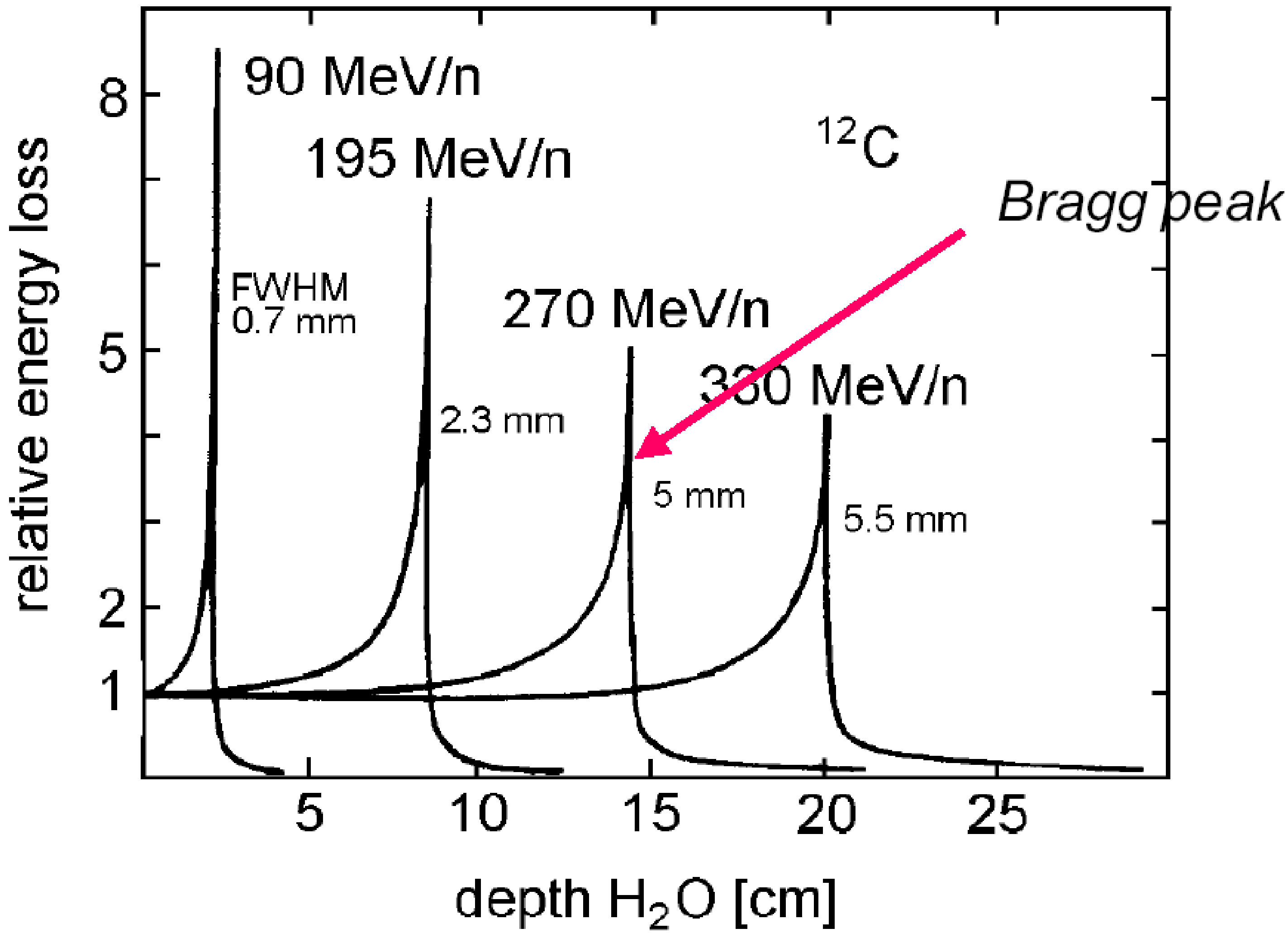

Bragg curves of ion beams

Inverted depth-dose profile

Unmodified Bragg peak

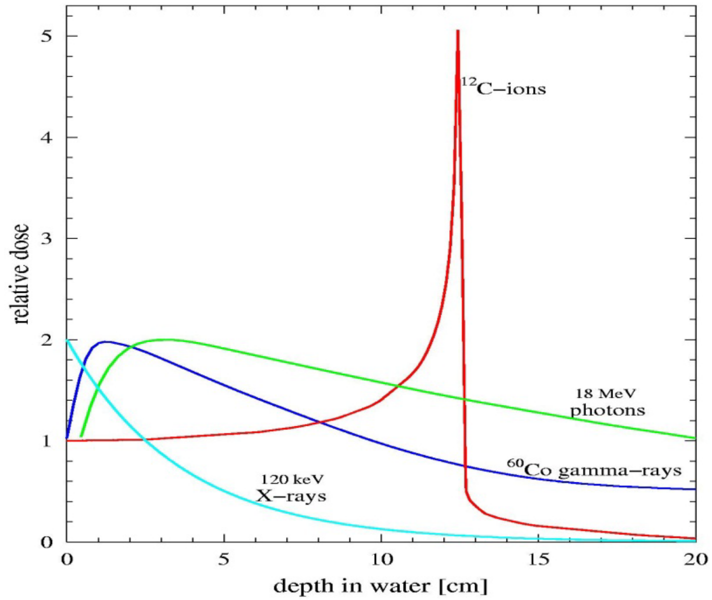

Extended target volume

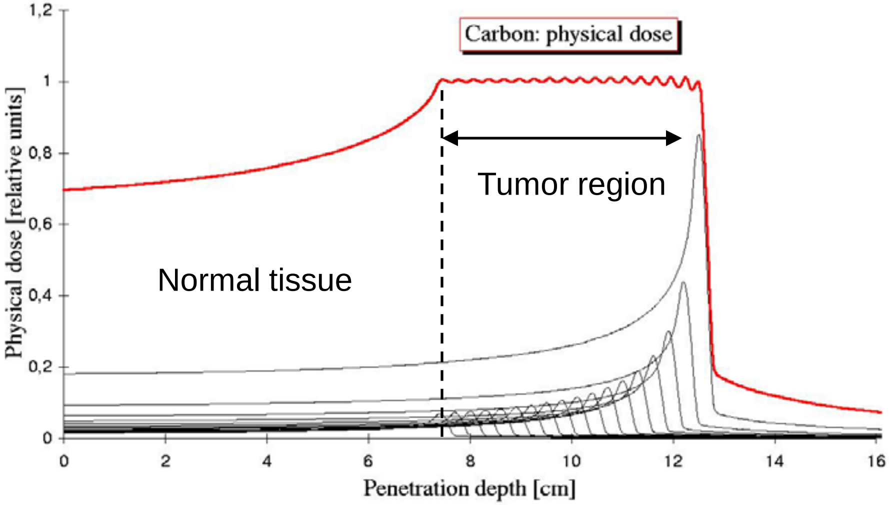

$$\frac{dE}{dx} = -4\pi N \frac{Z_P^2 e^4}{m_e c^2 \beta^2} Z_T \left[\ln \frac{2 m_e c^2 \beta^2}{I(1-\beta^2)} - \beta^2 \right]$$

Typically 30 energy steps needed

for a ripple < 5%

HELMHOLTZ | ASSOCIATION

Helmholtz Institute Jena

Bragg curves of ion beams

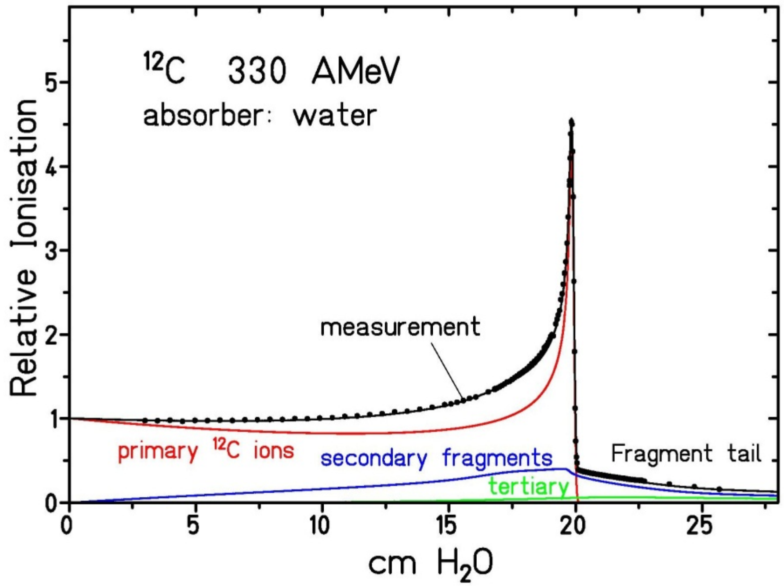

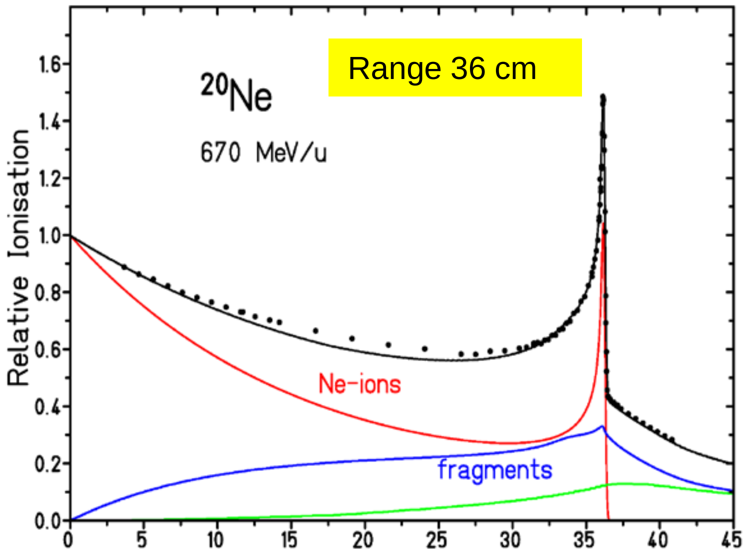

High-energy carbon beam stopping in water

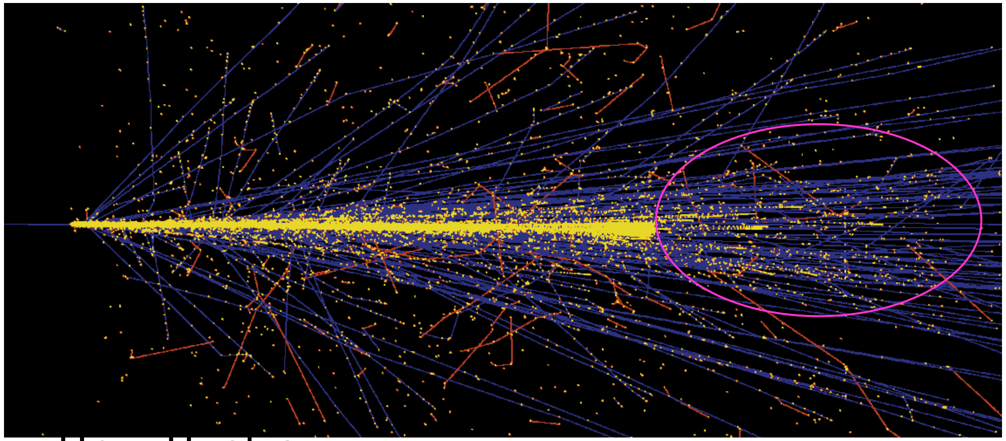

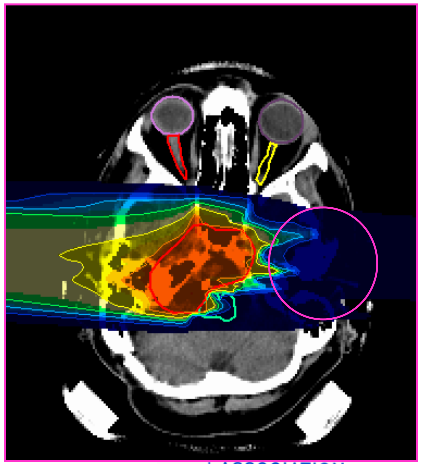

Comparision with other therapies

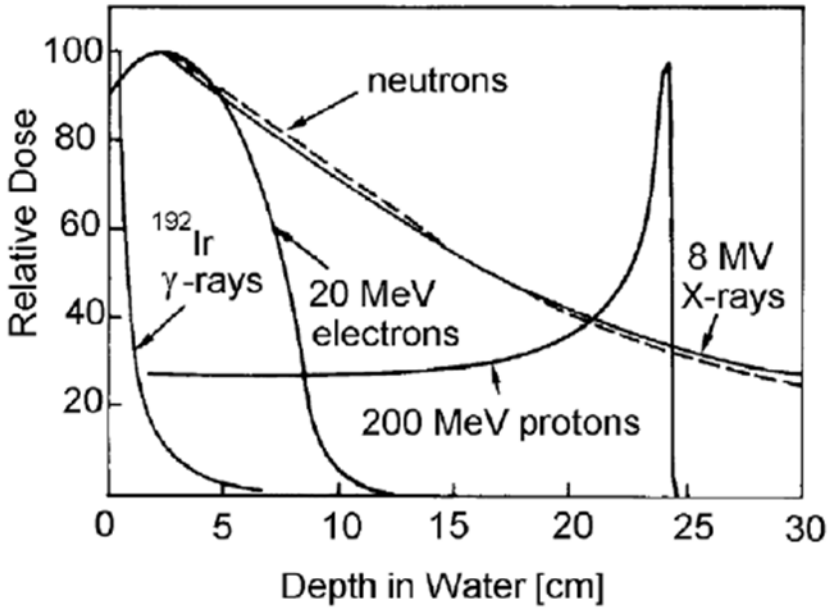

Tumortherapie mit ionisierenden Teilchenstrahlen:

- *γ-Strahler und hochenergetische Photonen*
  starke Absorbtion an Oberfläche
- *Elektronen*
  starke Absorbtion an Oberfläche
- *Neutronen*
  starke Absorbtion an Oberfläche
  Lokal: $n + {}^{10}B \rightarrow {}^{7}Li + \alpha$
- *Pionen π^- Sekundärstrahl:*
  $p + nukl \rightarrow p + nukl + \pi^+ + \pi^- + \pi^0$
- *Protonen*
- *Schwere Ionen*
  hohe biologische Wirksamkeit im Bragg peak

Microbeam - Irradiation of single cells

Nucleus of a human fibroblast cell

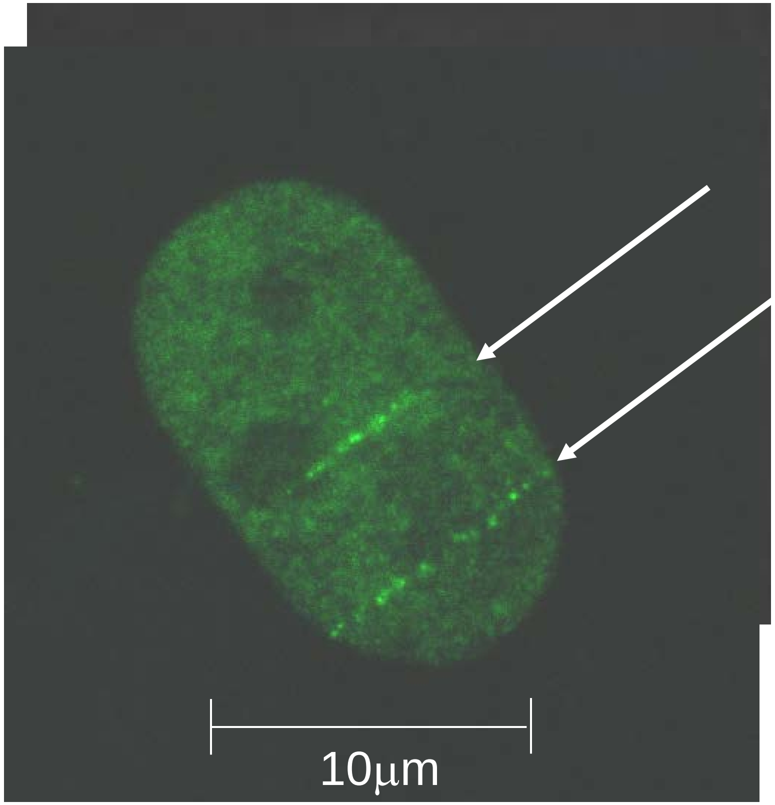

Jakob et al., Rad. Res.163,681(2005)

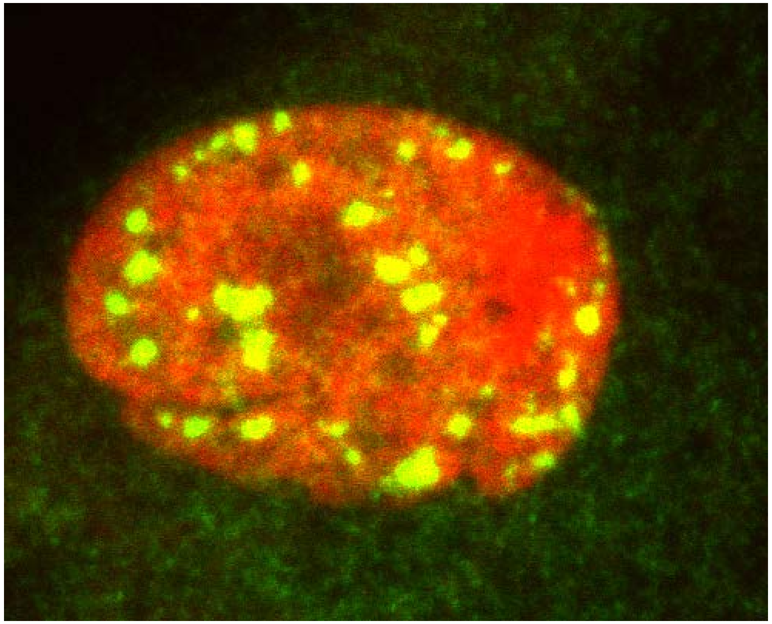

Biological response visualized by immuno-staining
Barberet et al, Rad. Res. 166,682(2006)

Biological effectivity

Increased biological effectivity of ions because of more DNA helix breaks.

Transversal range of the ionizing radiation:

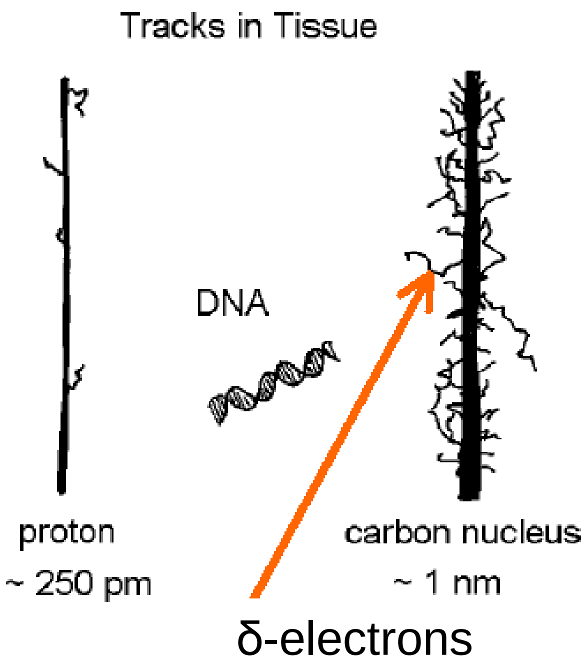

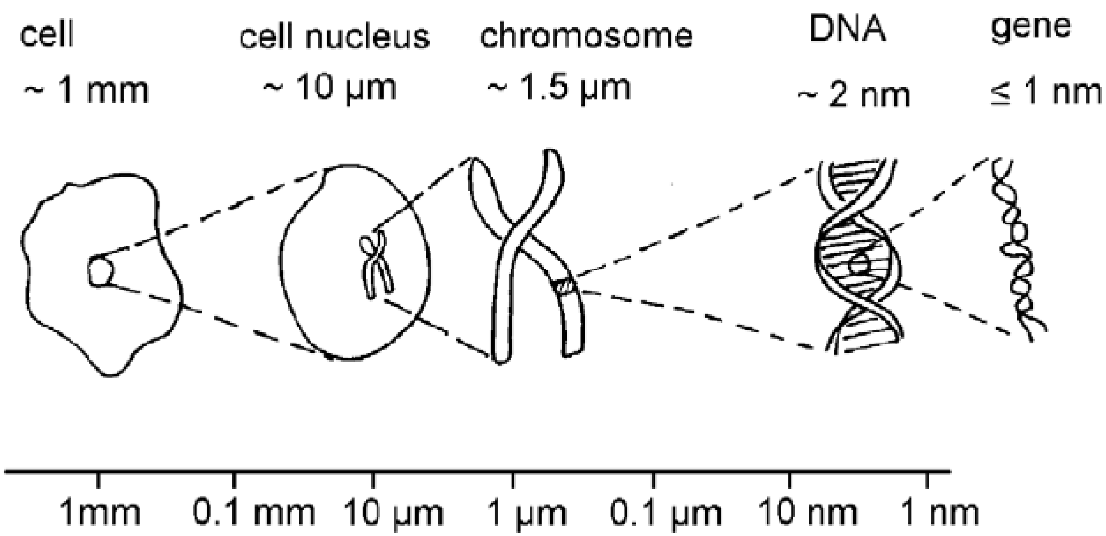

Biological effects of heavy ions
Tracks in cells

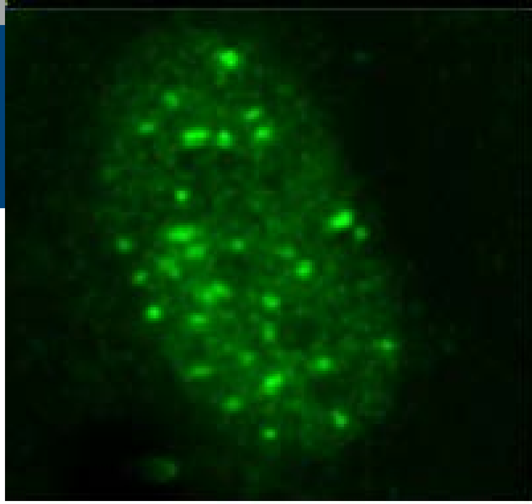

γ-rays

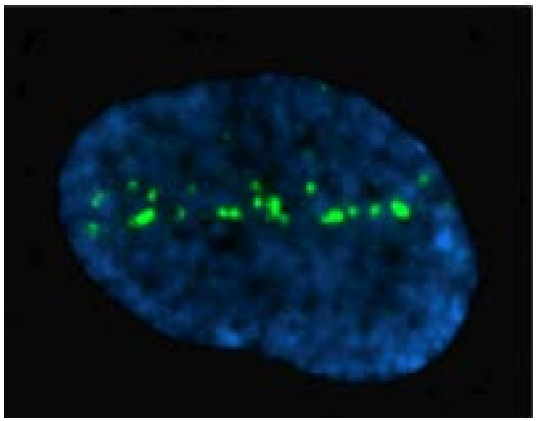

silicon

iron

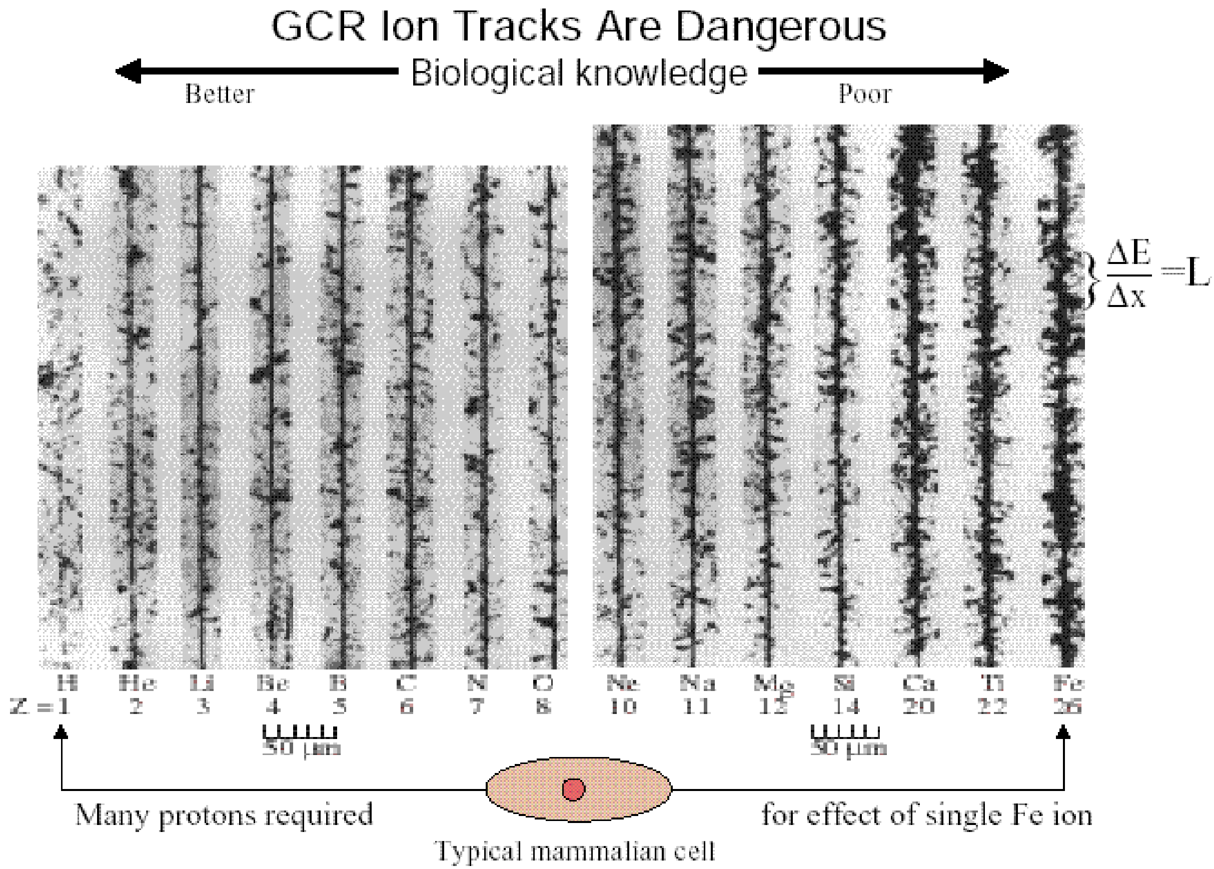

Cucinotta and Durante, *Lancet Oncol.* 2006

Heavy Ion Tracks Visualized in Human Cells

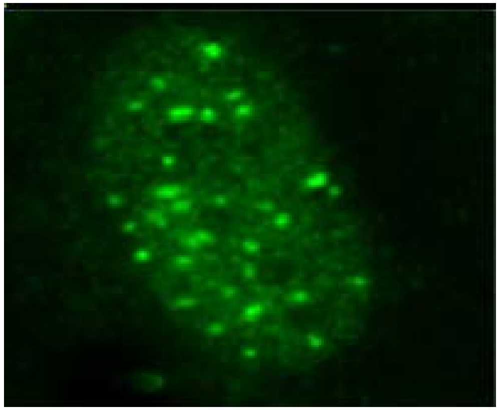

γ-rays

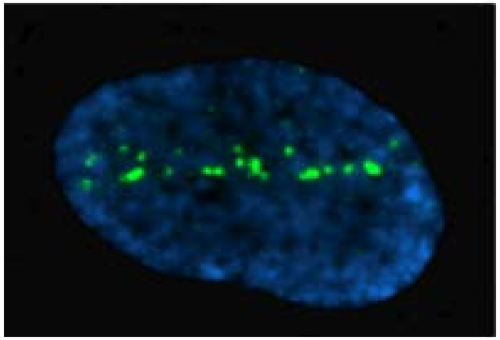

silicon

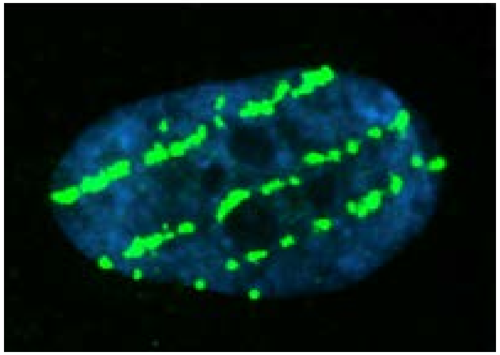

iron

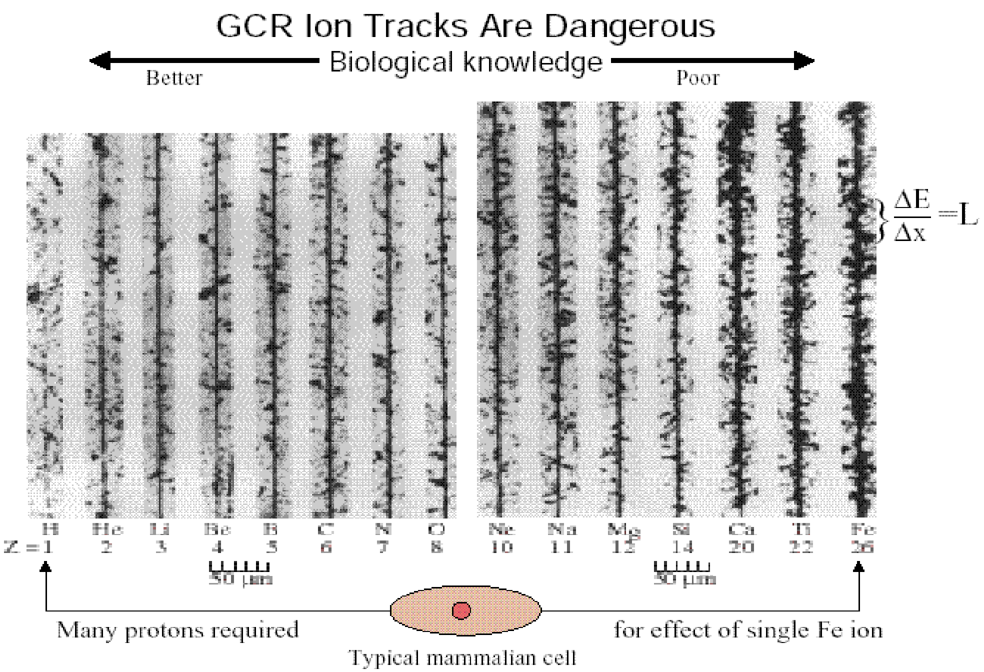

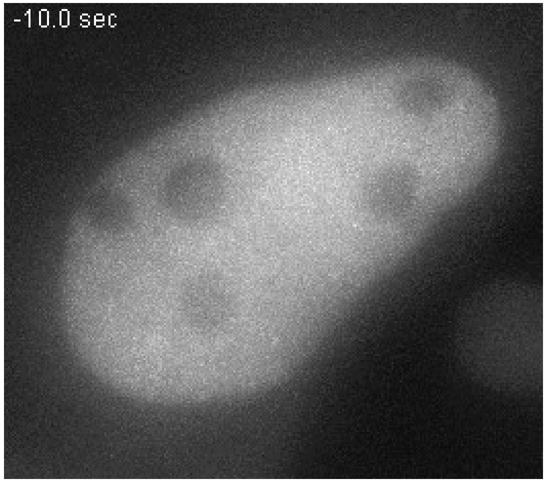

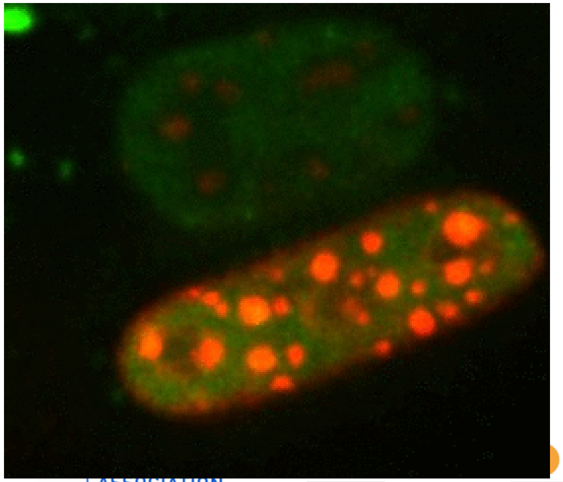

Beamline live cell imaging

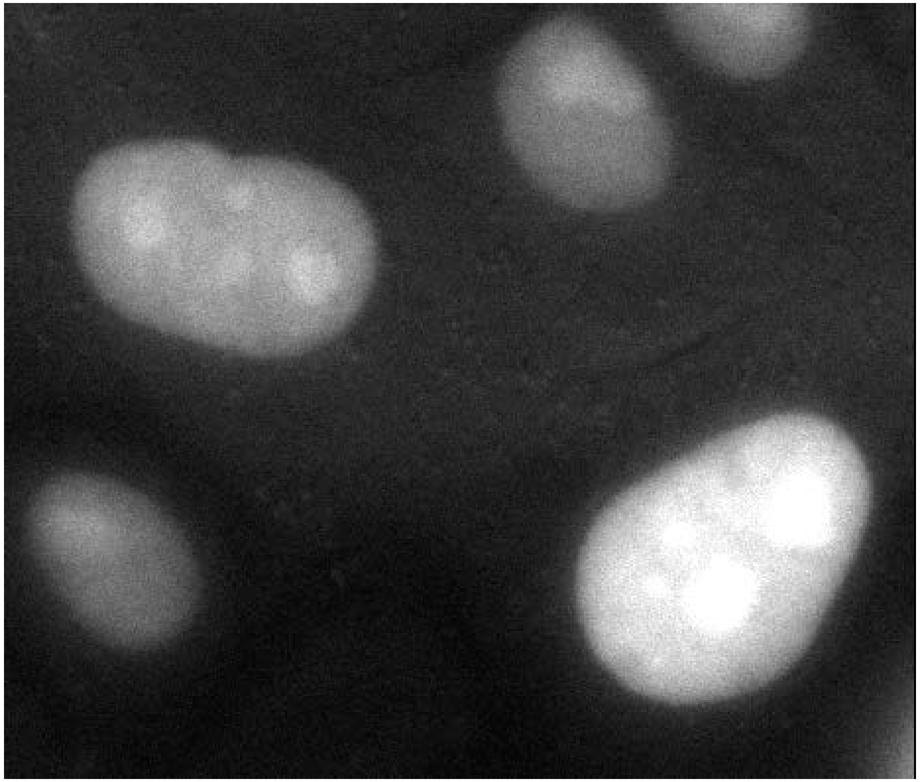

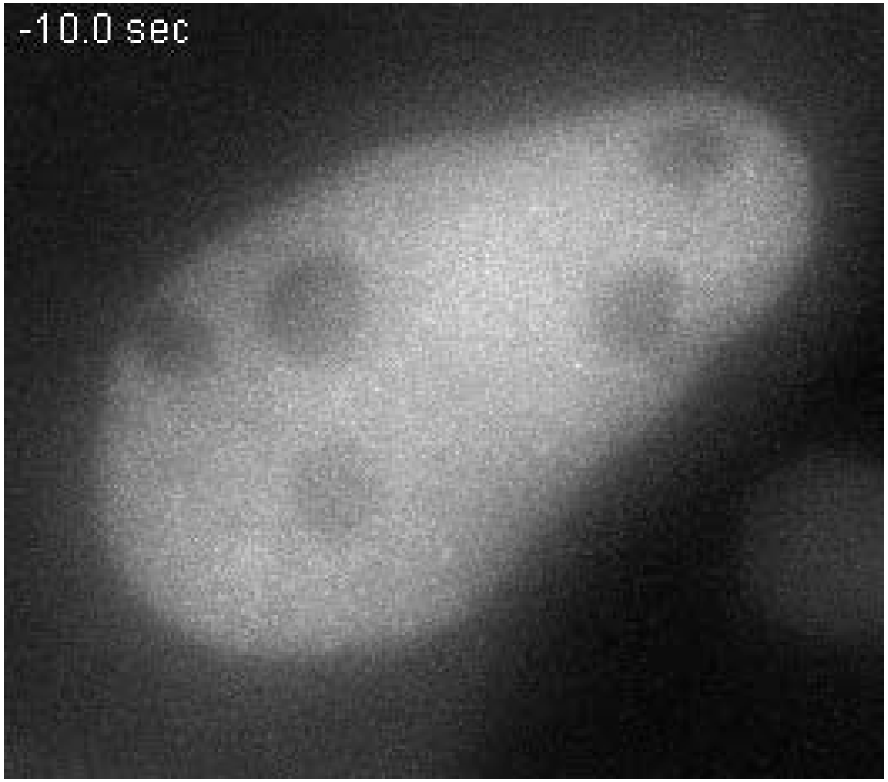

Uranium 11 MeV/n, 90°

Human cells

GFP- APTX (Aprataxin)

Jakob *et al. Proc. Natl. Acad. Sci. USA* (2009)

Iron 1 GeV/n, 0°

Human cells

GFP-Nijmegen breakage syndrome 1 (NBS1)

Chromosomal aberrations induced by heavy ions

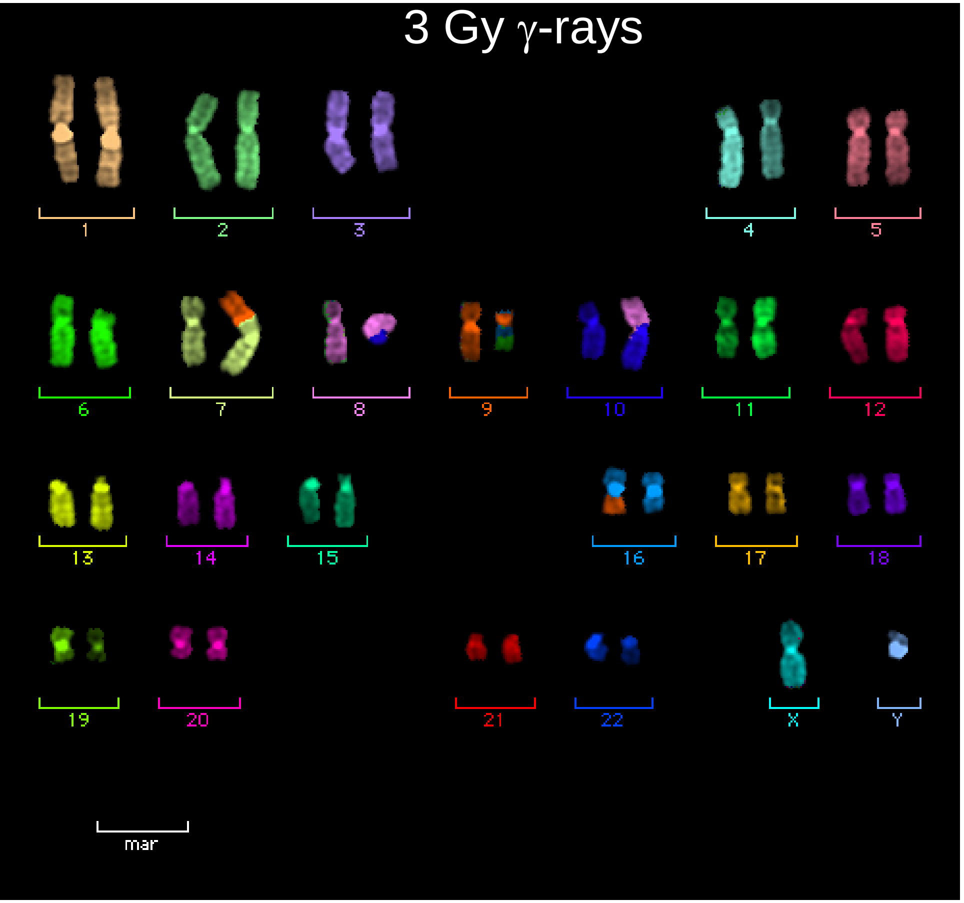

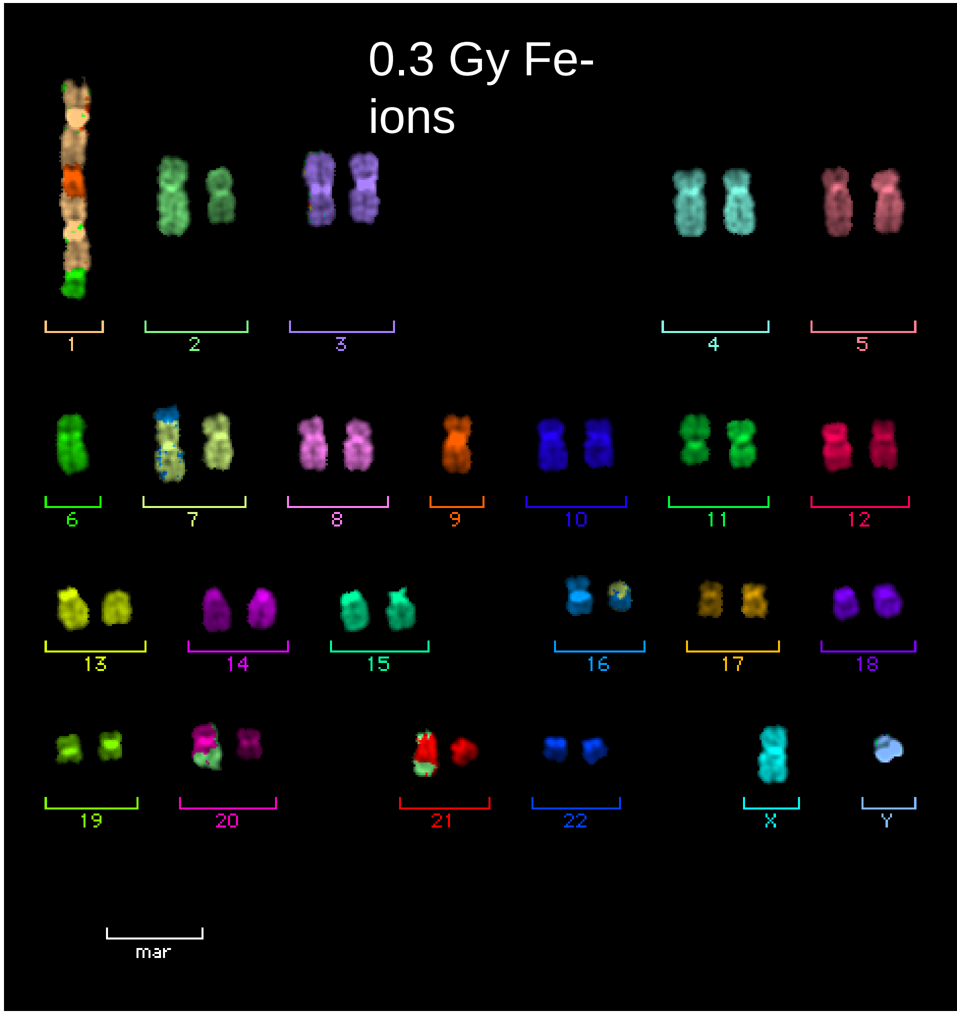

Durante *et al.*, *Radiation Research* 2002

Helmholtz Association
Helmholtz Institute Jena
GSI

Cell killing by different radiation types

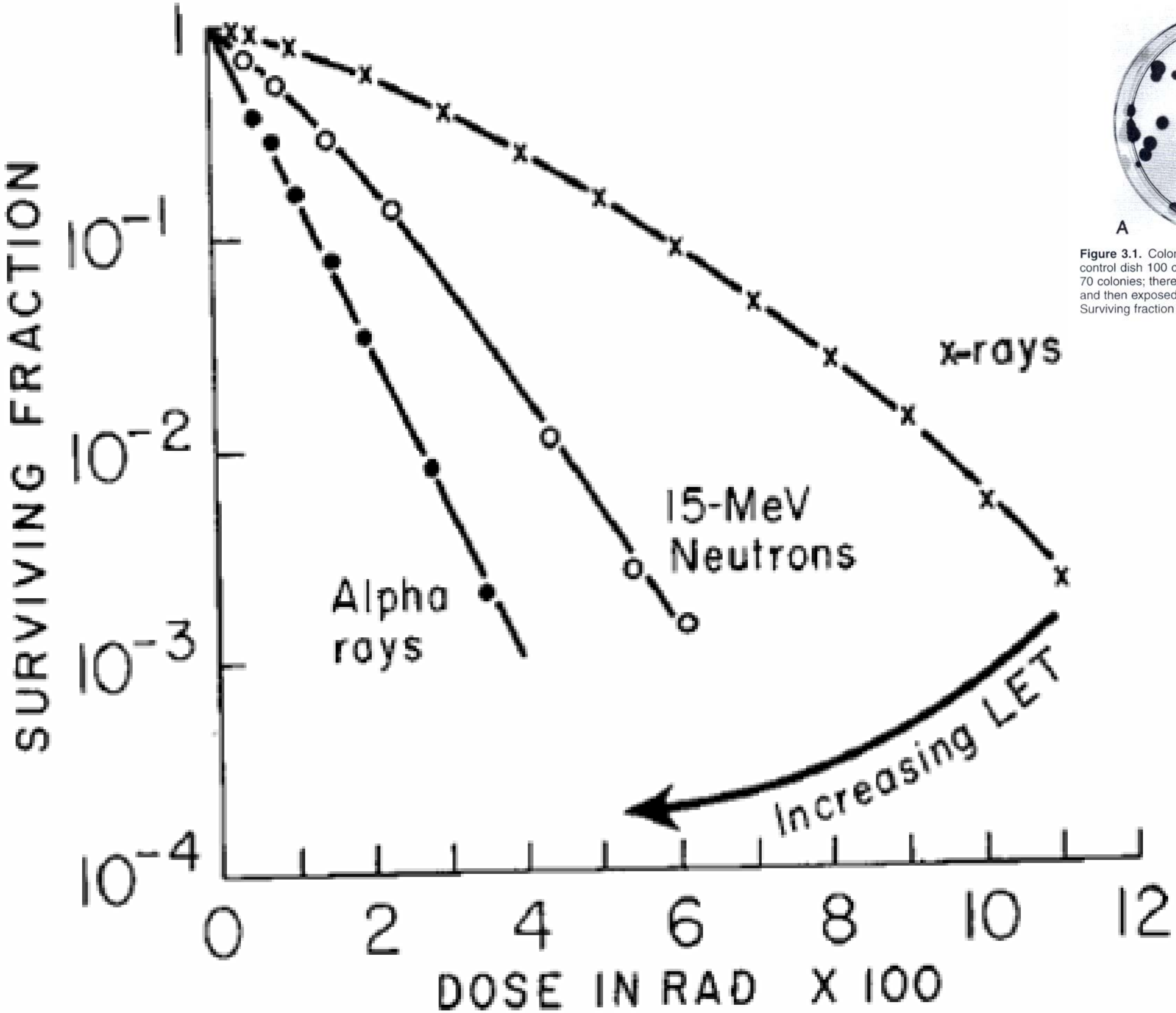

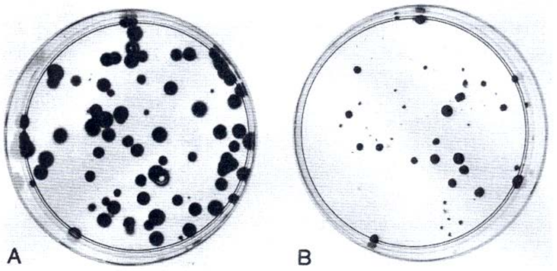

Figure 3.1. Colonies obtained with Chinese hamster cells cultured in vitro. **A:** In this unirradiated control dish 100 cells were seeded and allowed to grow for 7 days before being stained. There are 70 colonies; therefore the plating efficiency is 70/100, or 70%. **B:** Two thousand cells were seeded and then exposed to 800 rad (8 Gy) of x-rays. There are 32 colonies on the dish. Thus:
Surviving fraction = Colonies counted [colonies seeded x (PE/100)]
= 32/2000x .7
= 0.023

LET:
linear energy transfer

The good side of radiation: radiotherapy

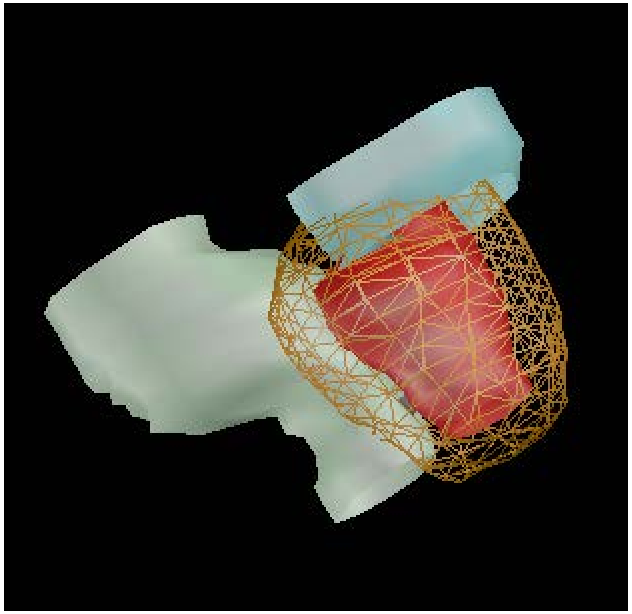

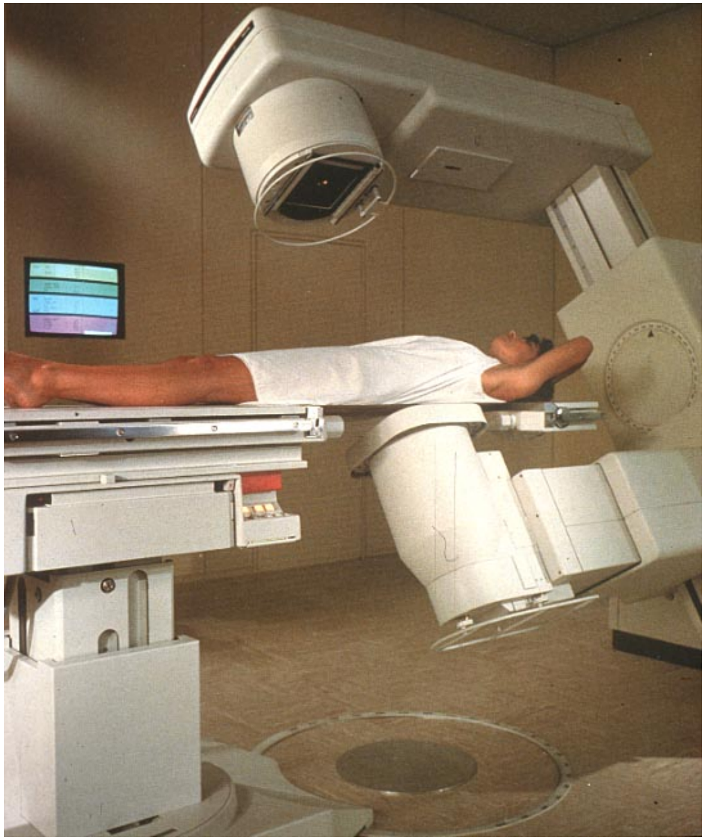

Task

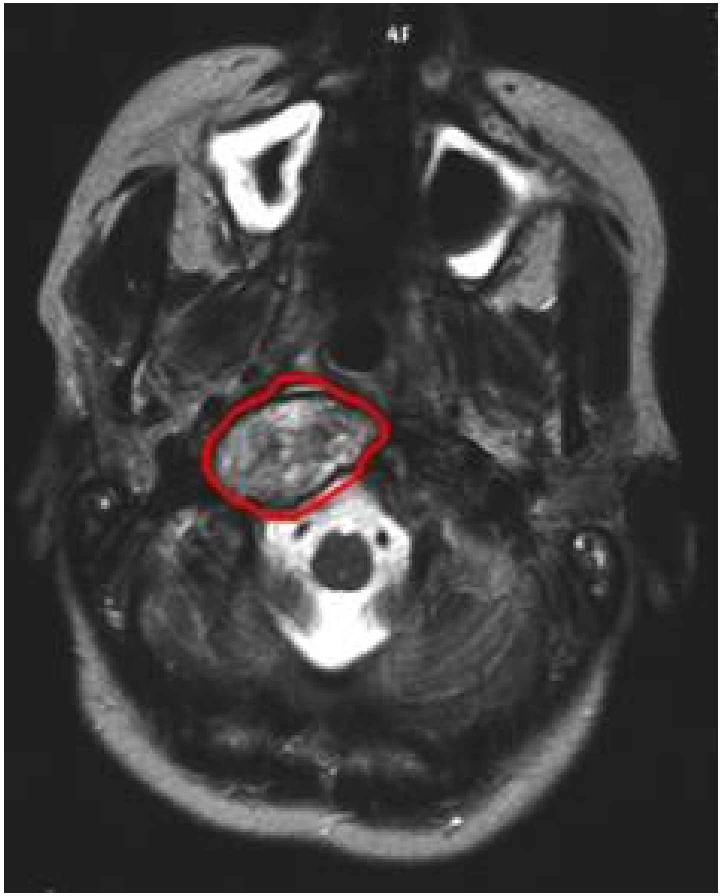

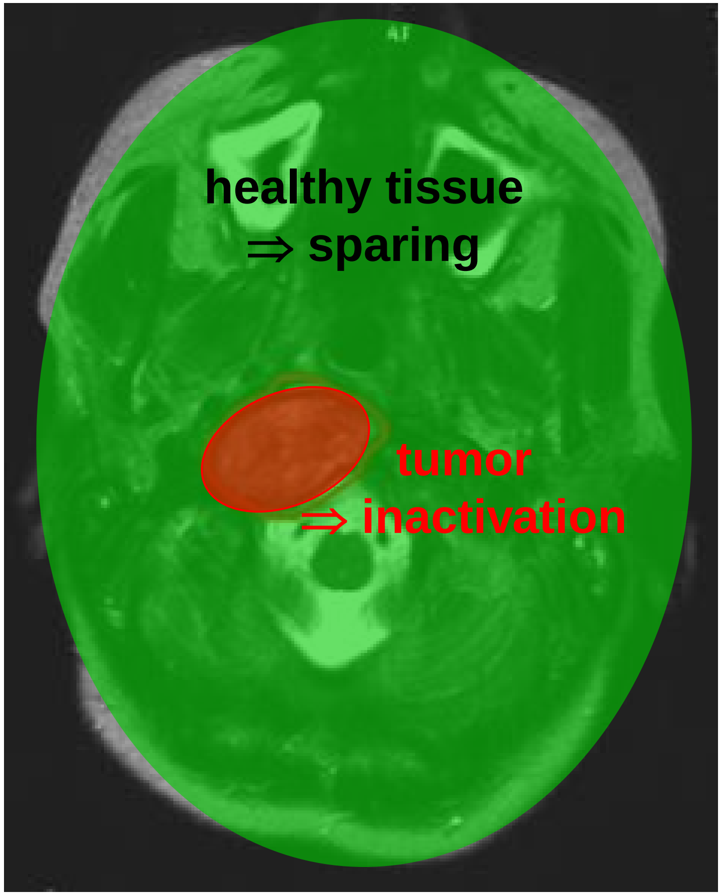

Tumor therapy: treatment strategy

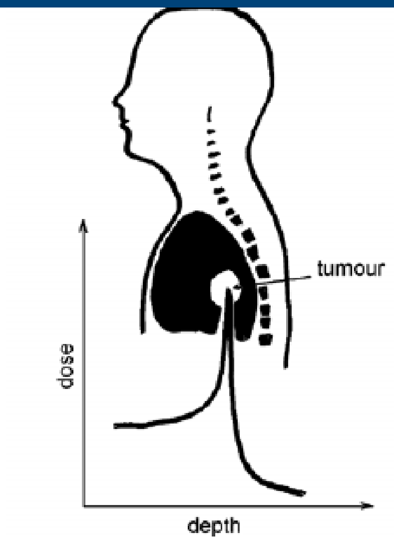

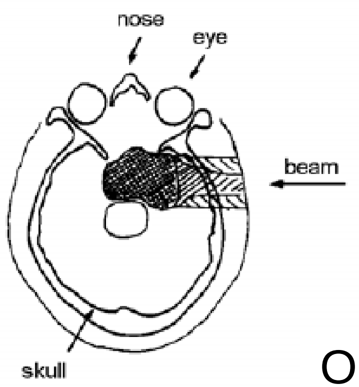

The treatment has to take care of size and precise location of the tumor. Different structures of tissue and the biological effectivity have to be taken into account.

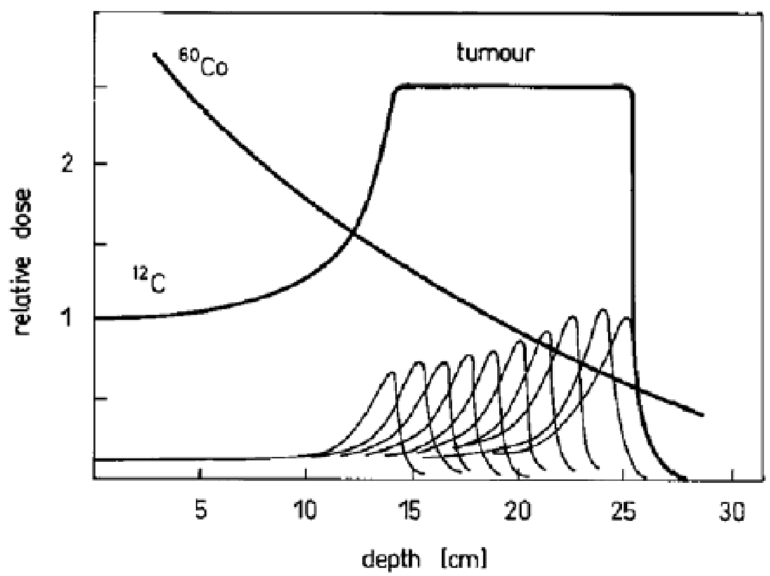

Observation of the location with positron emission tomography

- Fragmentation of ^{12}C produces ^{11,10}C
- β-decay:

  ^{10}C-> $^{10}B + \beta + \nu_e$ $T_{1/2}$=19.3 s

  ^{11}C-> $^{11}B + \beta^{+} + \nu_e$ $T_{1/2}$=20.38 min
- *Annihilation* $e^{+} + e^{-} \rightarrow \gamma + \gamma$
- Correlated emission back-to-back of two 511keV γ-quanta
- resolution ~ 2-3mm

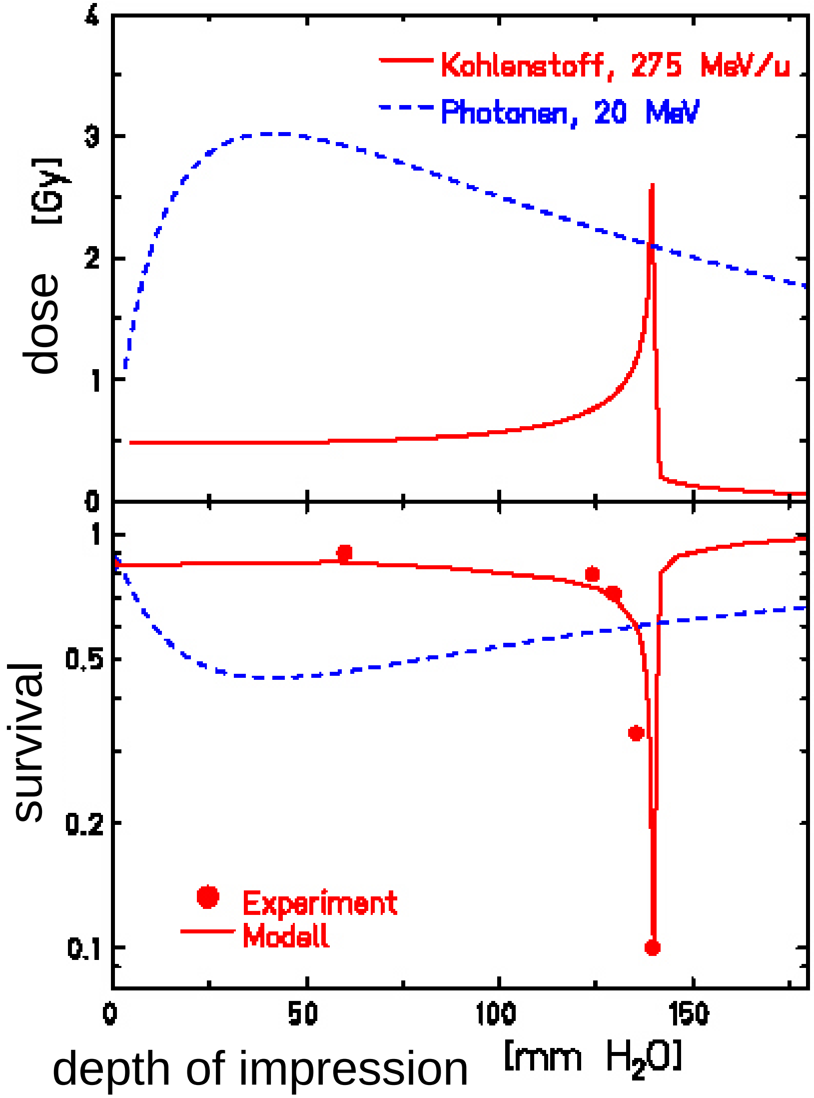

HELMHOLTZ ASSOCIATION
Helmholtz Institute Jena

Technical Realization

Intensity controlled Scan method

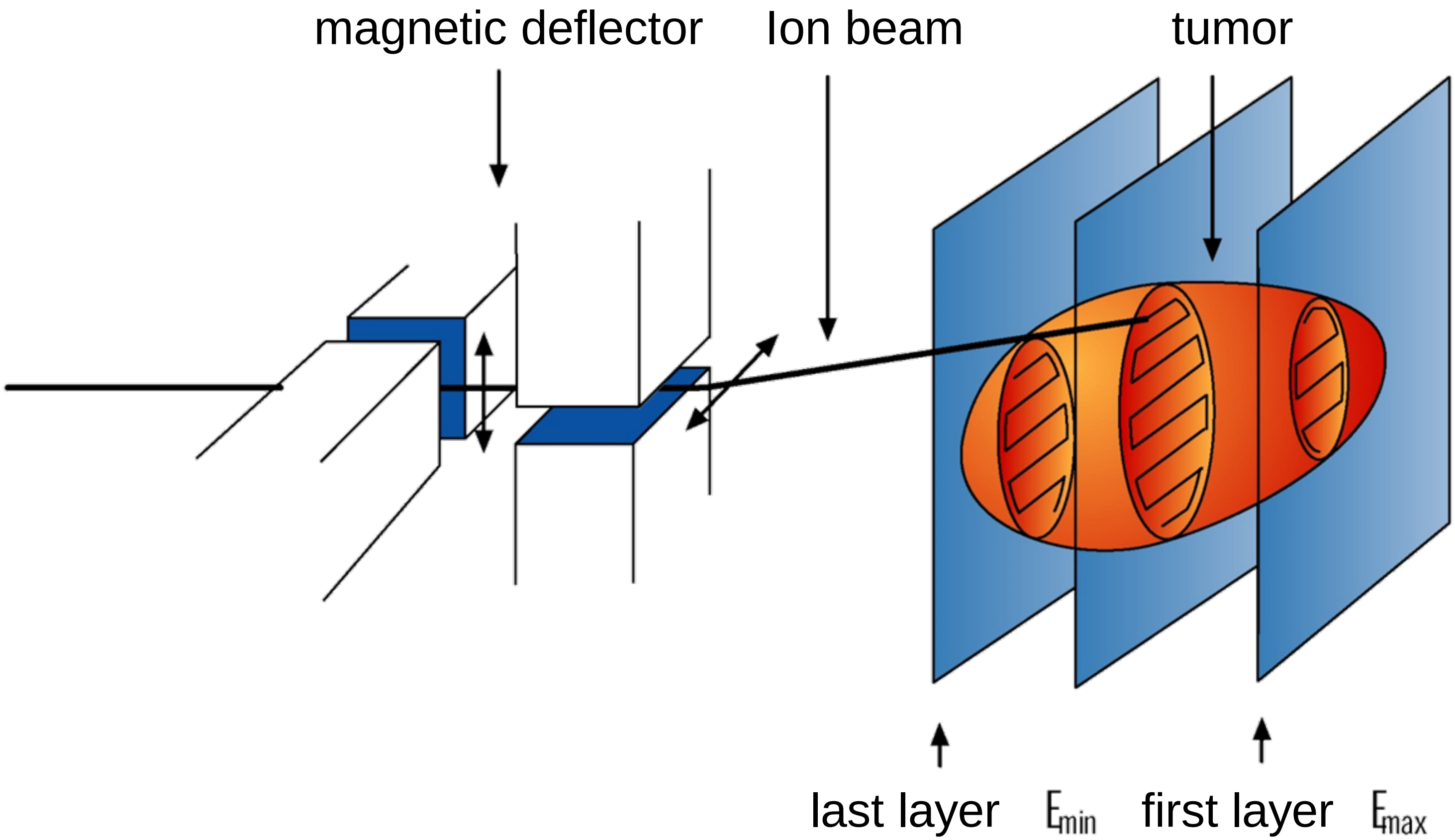

Scanned beam delivery – example / CR-39 stack

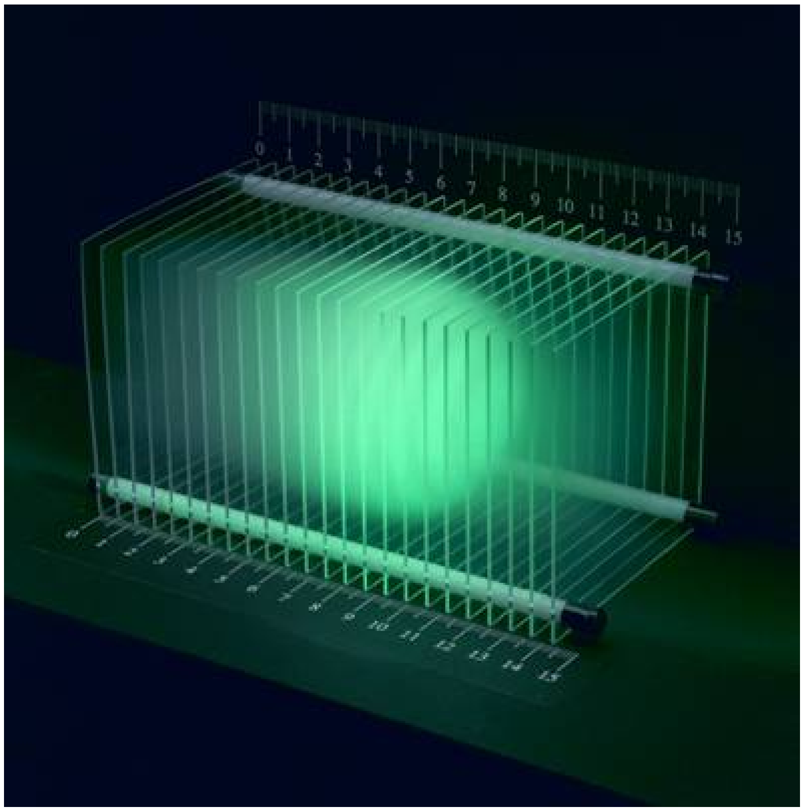

[M. Krämer, U. Weber, GSI and Phys. Med. Biol. 2000]

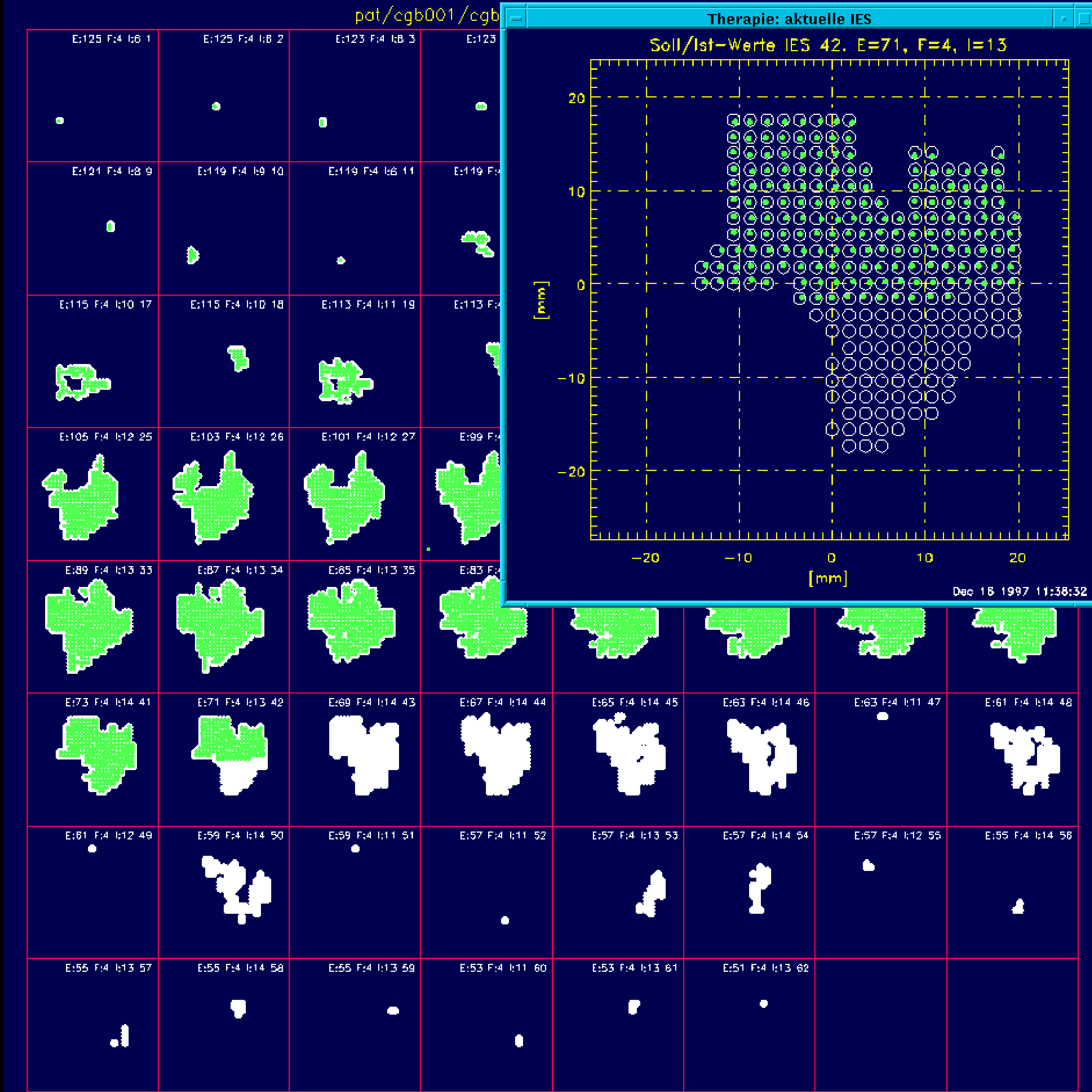

pat/cgb001/cgb
E:125 F:4 I:6 1
E:125 F:4 I:8 2
E:123 F:4 I:8 3
E:123
E:121 F:4 I:8 9
E:119 F:4 I:9 10
E:119 F:4 I:6 11
E:119 F:
E:115 F:4 I:10 17
E:115 F:4 I:10 18
E:113 F:4 I:11 19
E:113 F:
E:105 F:4 I:12 25
E:103 F:4 I:12 26
E:101 F:4 I:12 27
E:99 F:
E:89 F:4 I:13 33
E:87 F:4 I:13 34
E:85 F:4 I:13 35
E:83 F:
E:73 F:4 I:14 41
E:71 F:4 I:13 42
E:69 F:4 I:14 43
E:67 F:4 I:14 44
E:65 F:4 I:14 45
E:63 F:4 I:14 46
E:63 F:4 I:11 47
E:61 F:4 I:14 48
E:61 F:4 I:12 49
E:59 F:4 I:14 50
E:59 F:4 I:11 51
E:57 F:4 I:11 52
E:57 F:4 I:13 53
E:57 F:4 I:14 54
E:57 F:4 I:12 55
E:55 F:4 I:14 56
E:55 F:4 I:13 57
E:55 F:4 I:14 58
E:55 F:4 I:13 59
E:53 F:4 I:11 60
E:53 F:4 I:13 61
E:51 F:4 I:13 62
Therapie: aktuelle IES
Soll/Ist-Werte IES 42. E=71, F=4, I=13
20
10
0
−10
−20
[mm]
−20
−10
0
10
20
[mm]
Dec 16 1997 11:38:32

Röntgenröhre

Bildverstärker

Patientenmaske

Strahlaustrittsfenster

Patientenmonitor

Patient

PET-Kamera

Patiententisch

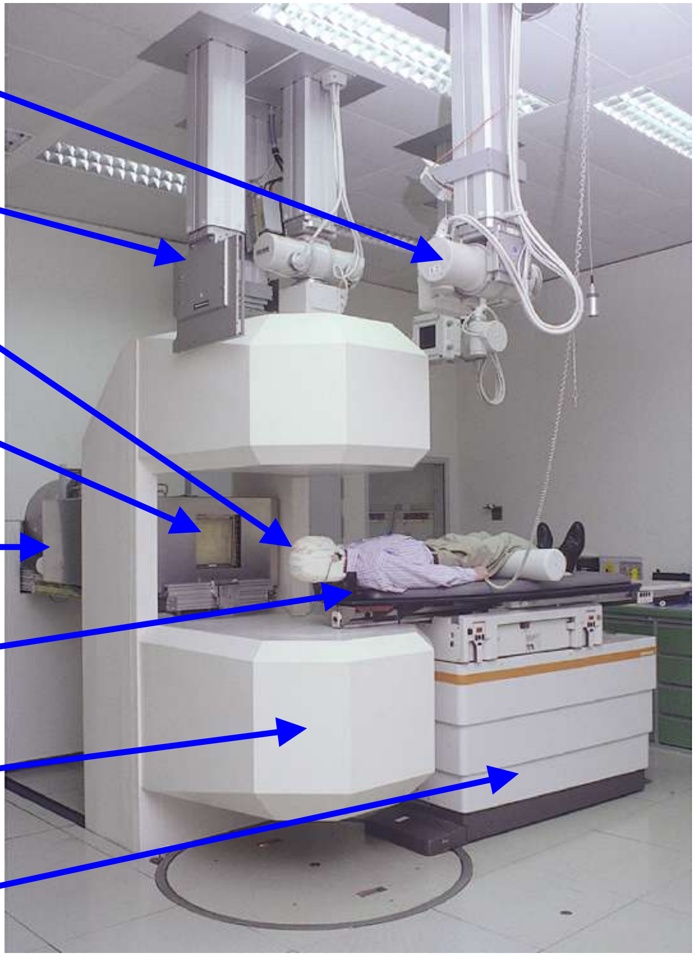

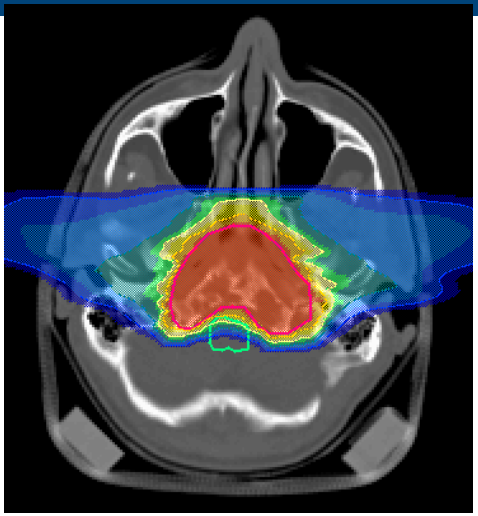

Here the distribution of the physical dose is shown overlapping with a CT picture of the brain
(red means high dose).
The dose will be optimized to gain a homogenous biological equivalent dose.

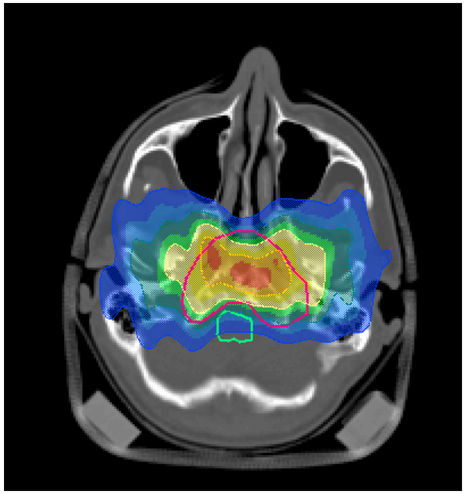

Distribution of the positron emitter measured with the PET-Camera. The maximum activity of the distribution is shifted to the border.
PET is sensitive to ^{11}C and ^{10}C nuclei.

Example of the course of disease: Tumor patient after therapy with carbon ions

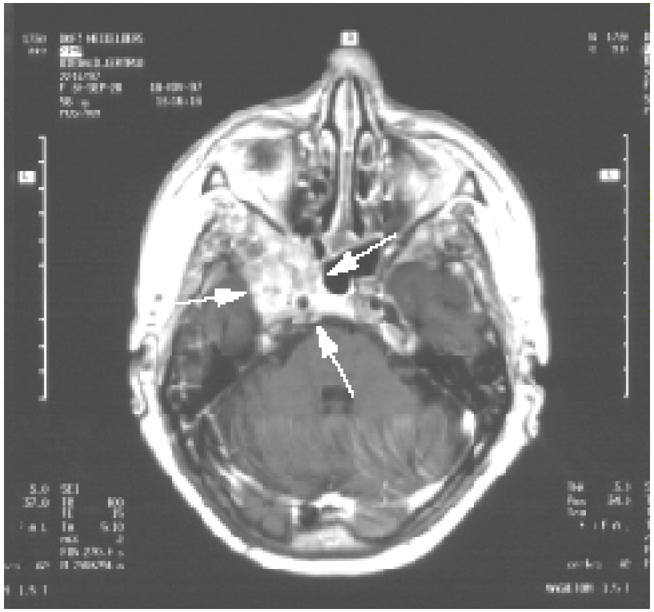

Before treatment:
Tumor at the base of the skull

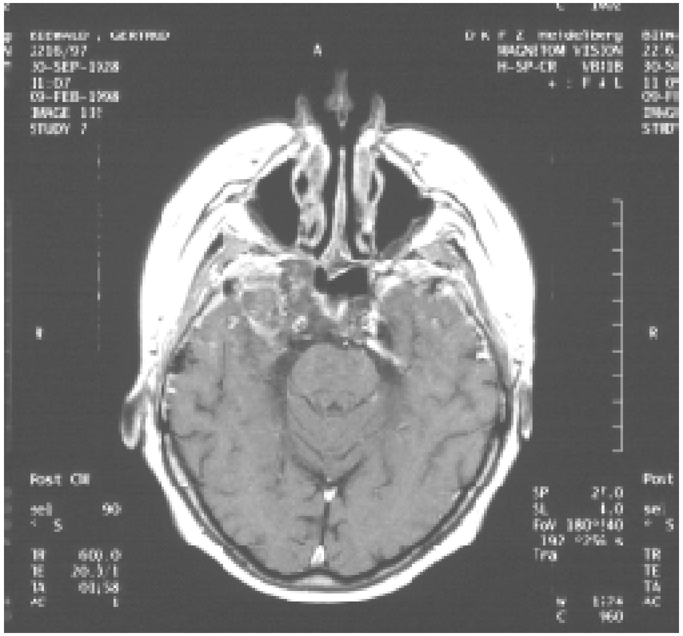

After the ion therapy

Target Motion and Volume Conformity

- volume conformal irradiation requires precise knowledge of target location

- active beam delivery: strong interferences between scanning and target motion

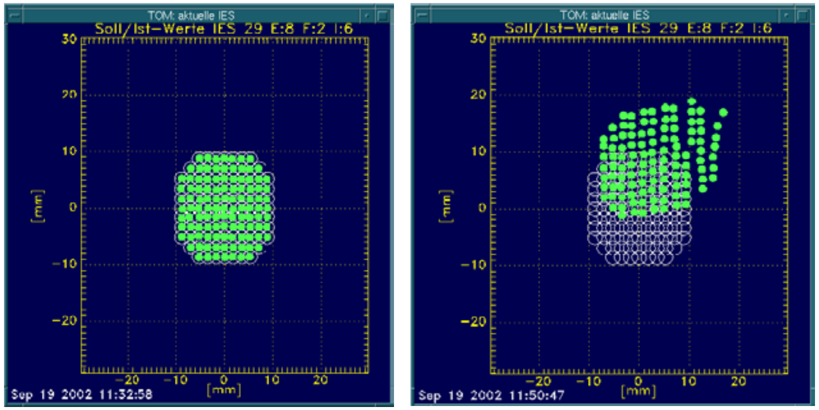

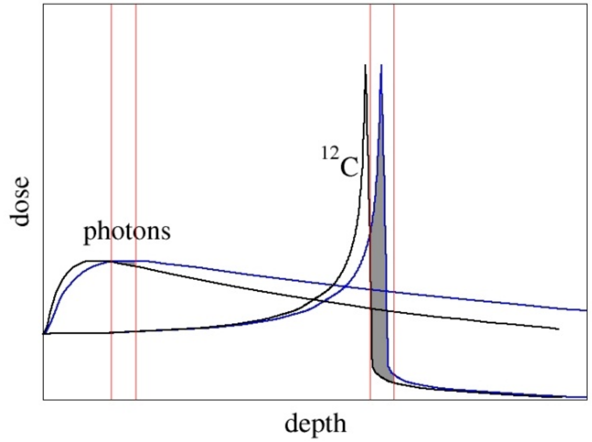

- charged particles: sensitivity in all three dimensions

HELMHOLTZ ASSOCIATION
Helmholtz Institute Jena
GSI

Tumor response to treatment

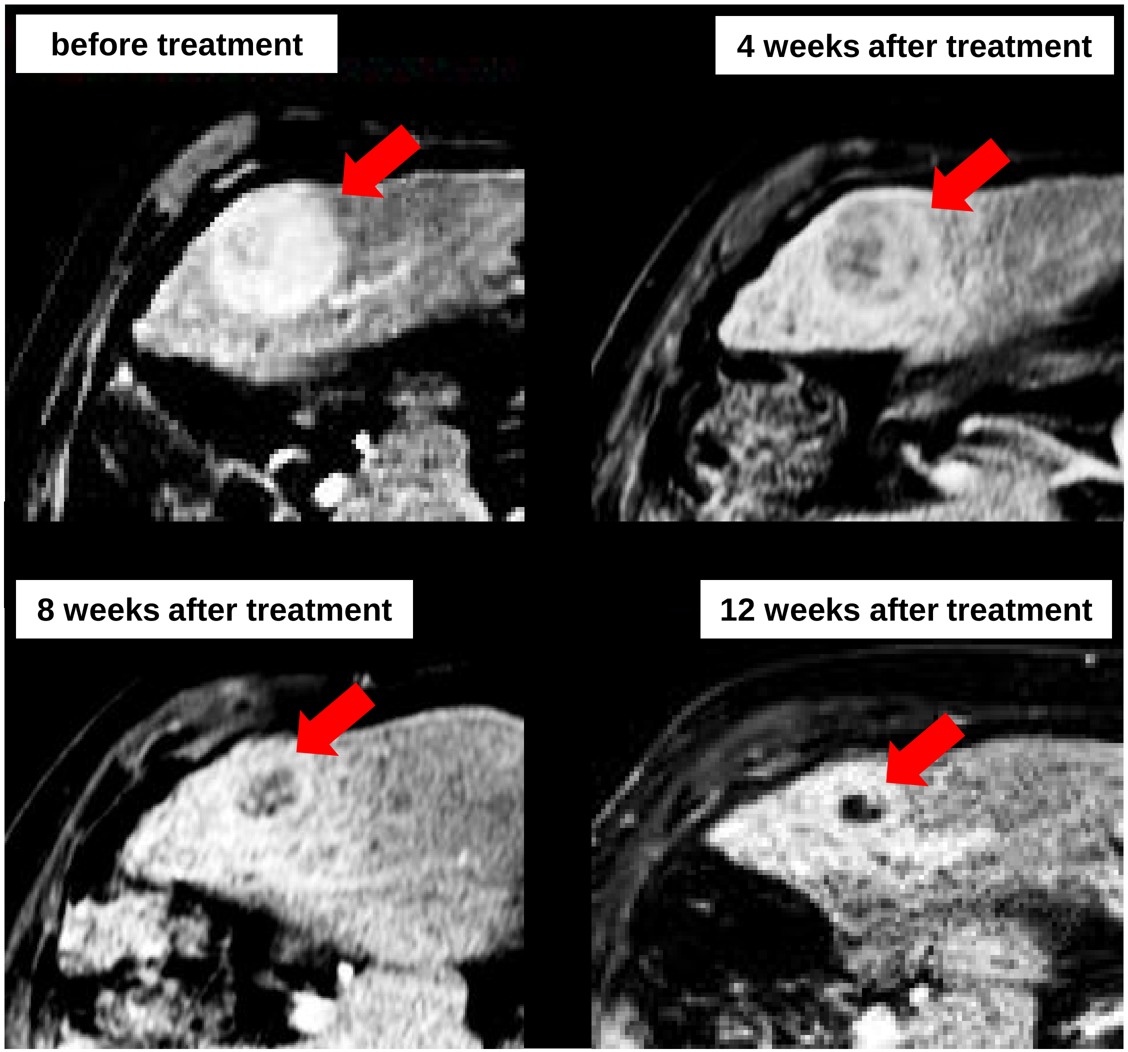

MRT images
of a treated patient

irradiation under
abdominal compression

⇒ visible tumor regression

[courtesy of
D. Habermehl et al., HIT]

Respiratory motion - beam range

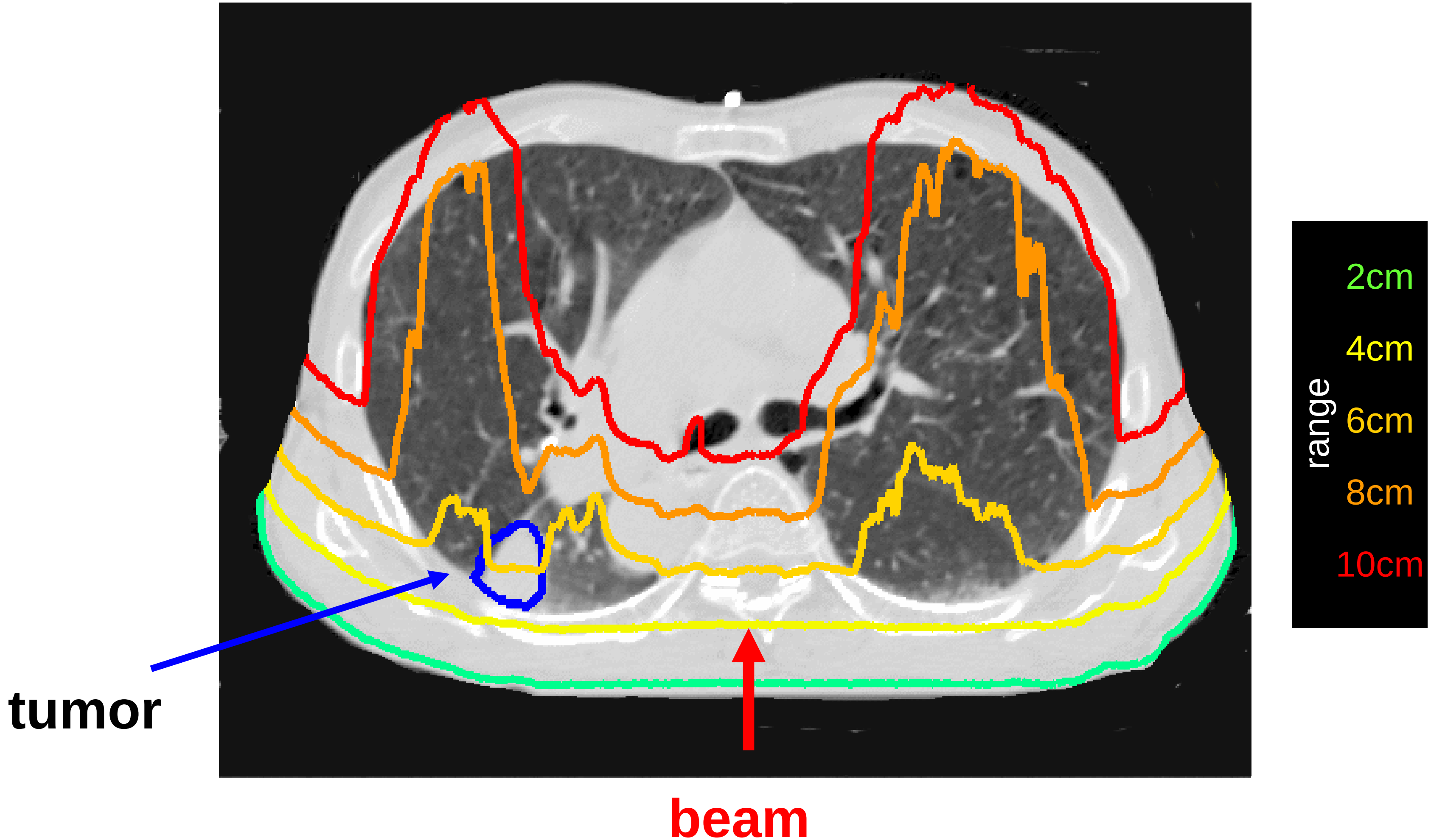

Problem of moving organs

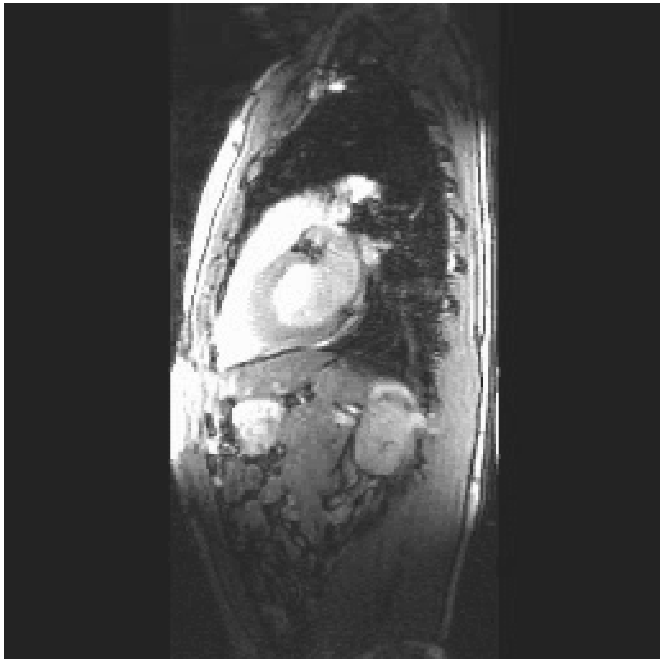

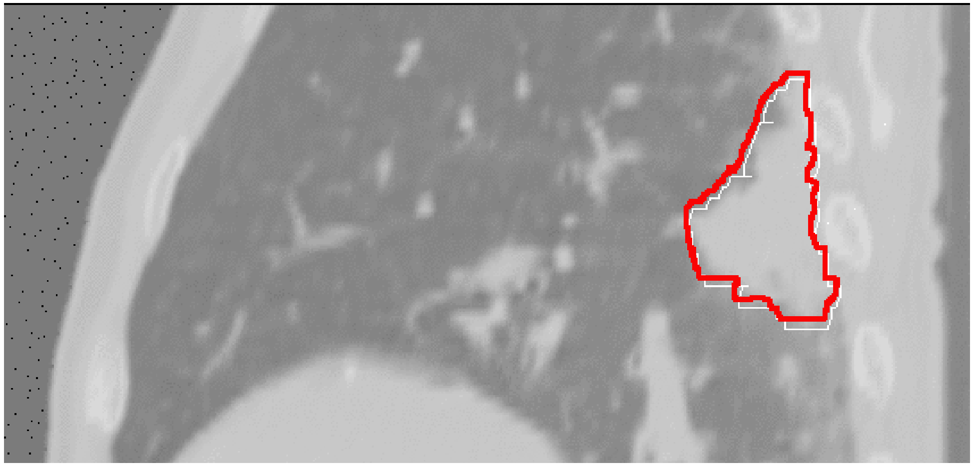

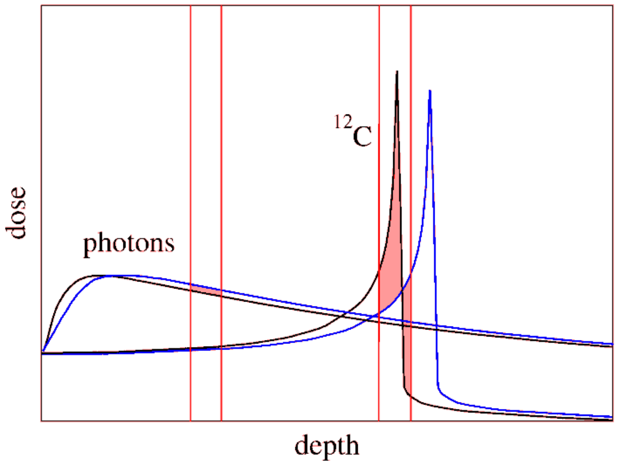

for ions: variations in radiological path length extremely important

Motion monitoring

(External) motion surrogate

Internal motion

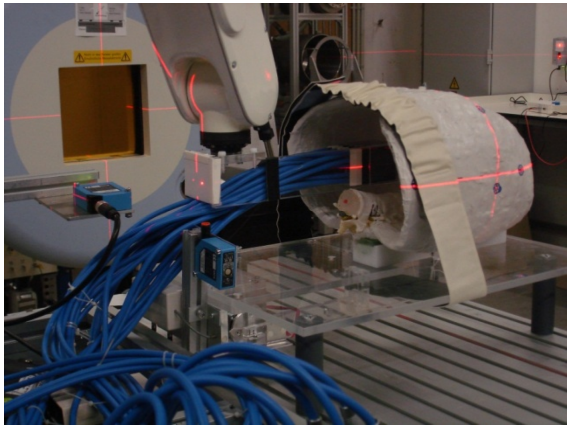

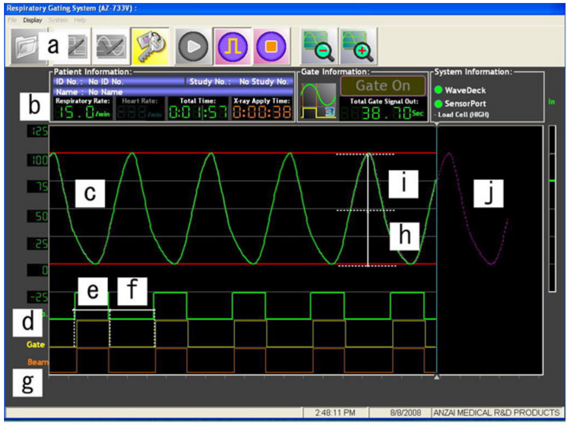

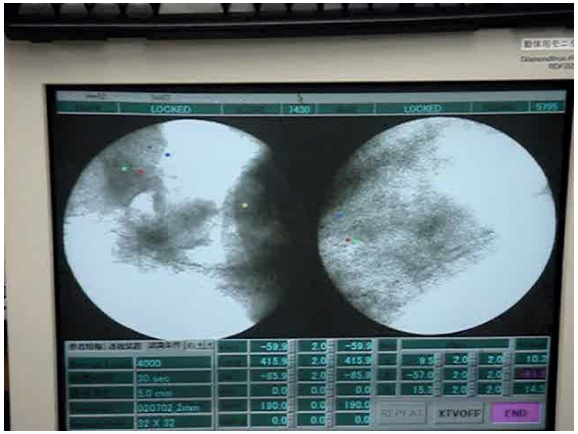

limited precision

invasive

combine advantages by correlation models (e.g., artificial neural networks, ANN)

Helmholtz Institute Jena

3D online motion compensation

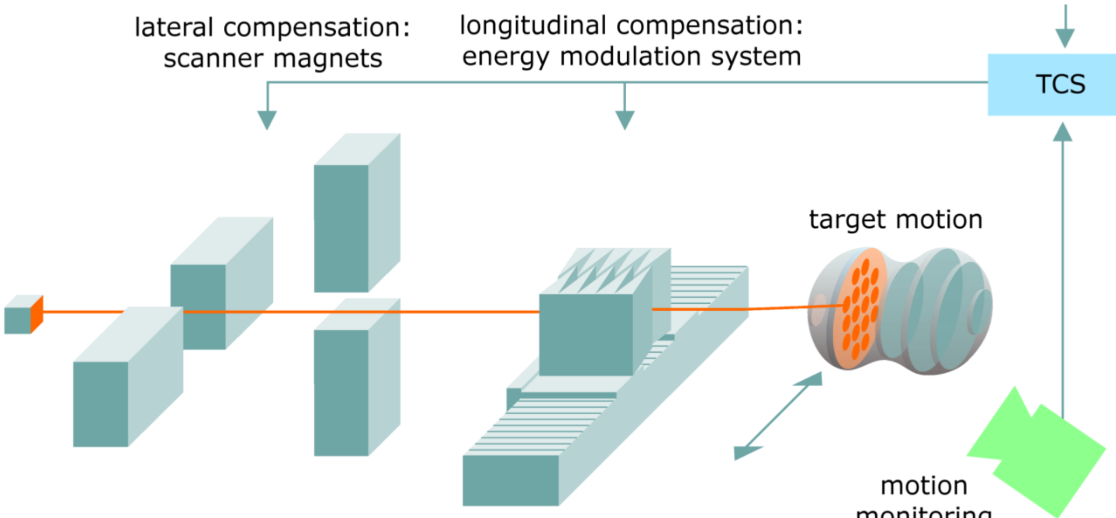

magnetic scanner system

PMMA wedge system

suitable motion tracking system

dynamic treatment plan

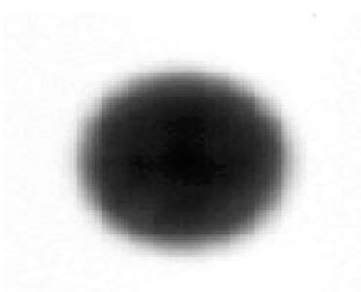

static

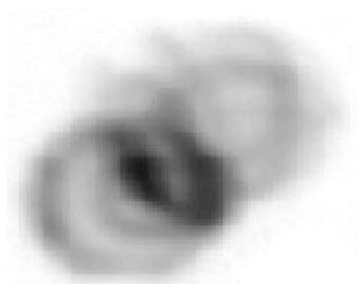

moving, non-compensated

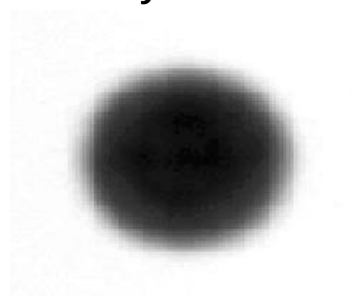

moving, compensated

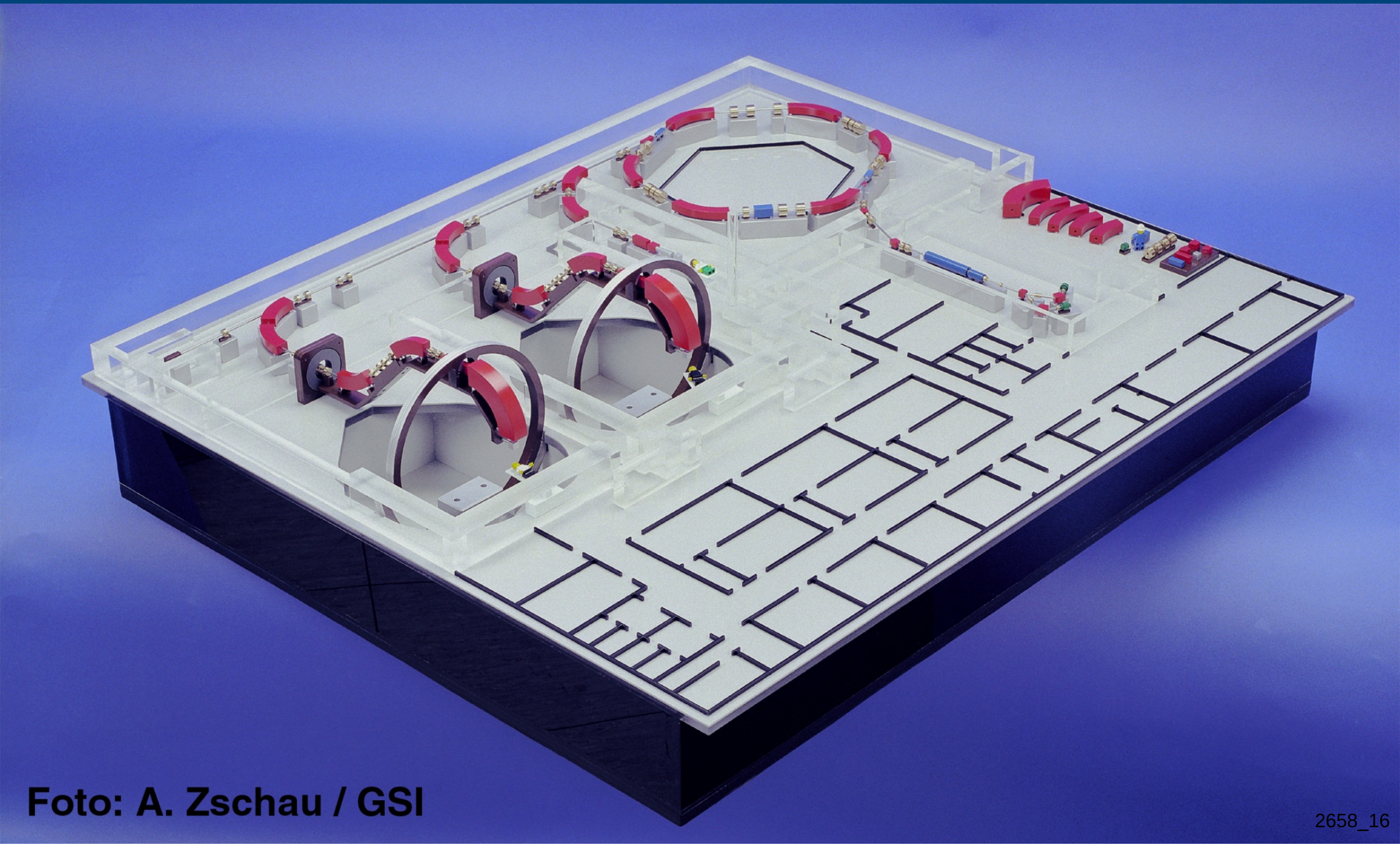

Foto: A. Zschau / GSI

2658_16

HIT
Heidelberger Ionenstrahl-Therapiezentrum

UniversitätsKlinikum Heidelberg

IonenStrahl TherapieZentrum

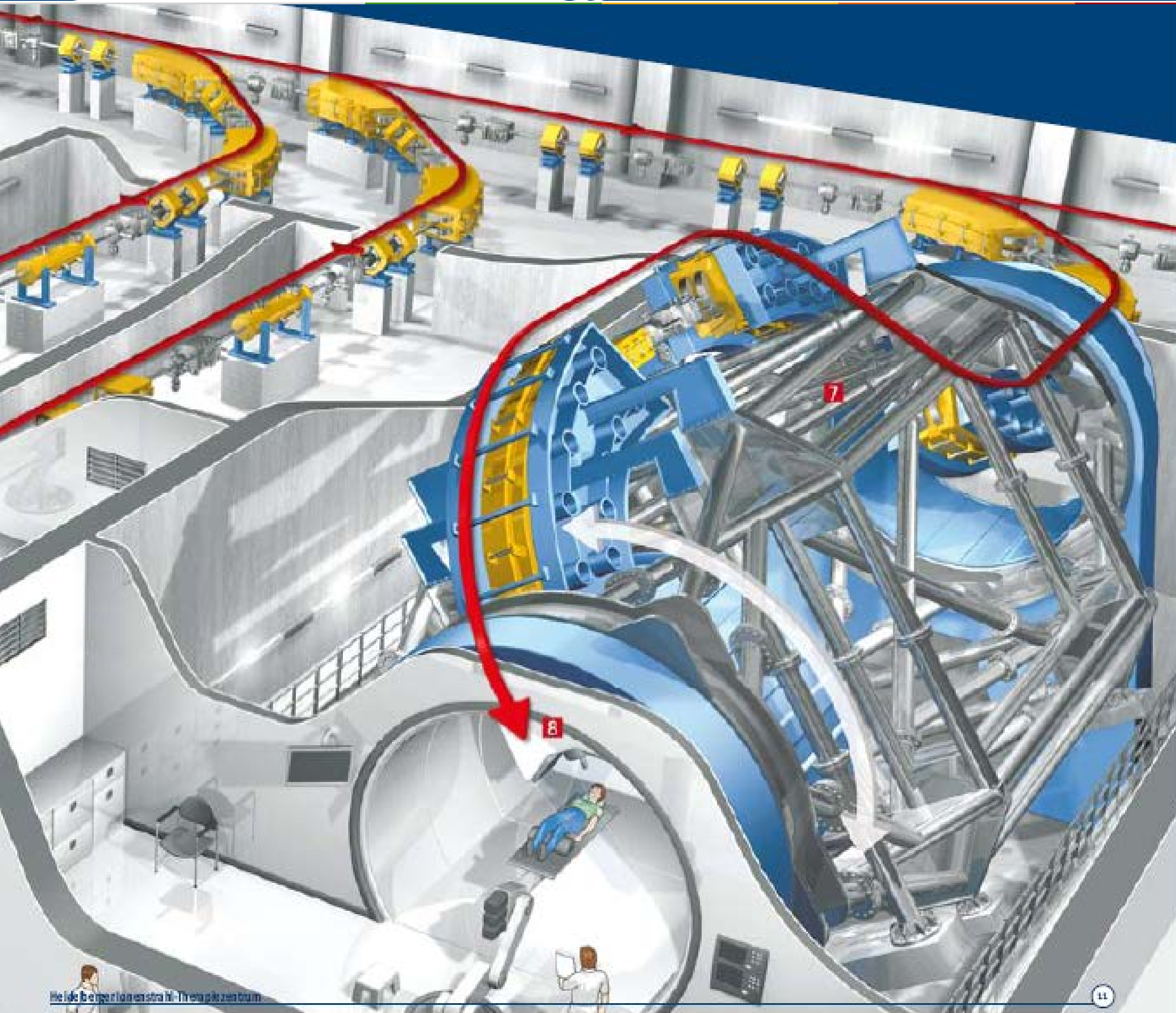

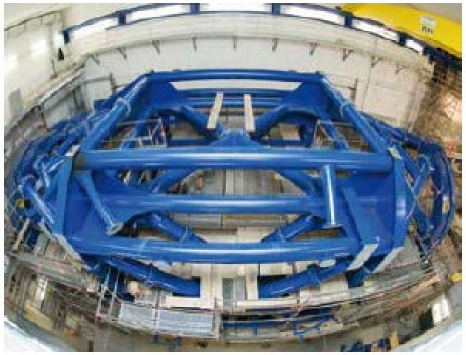

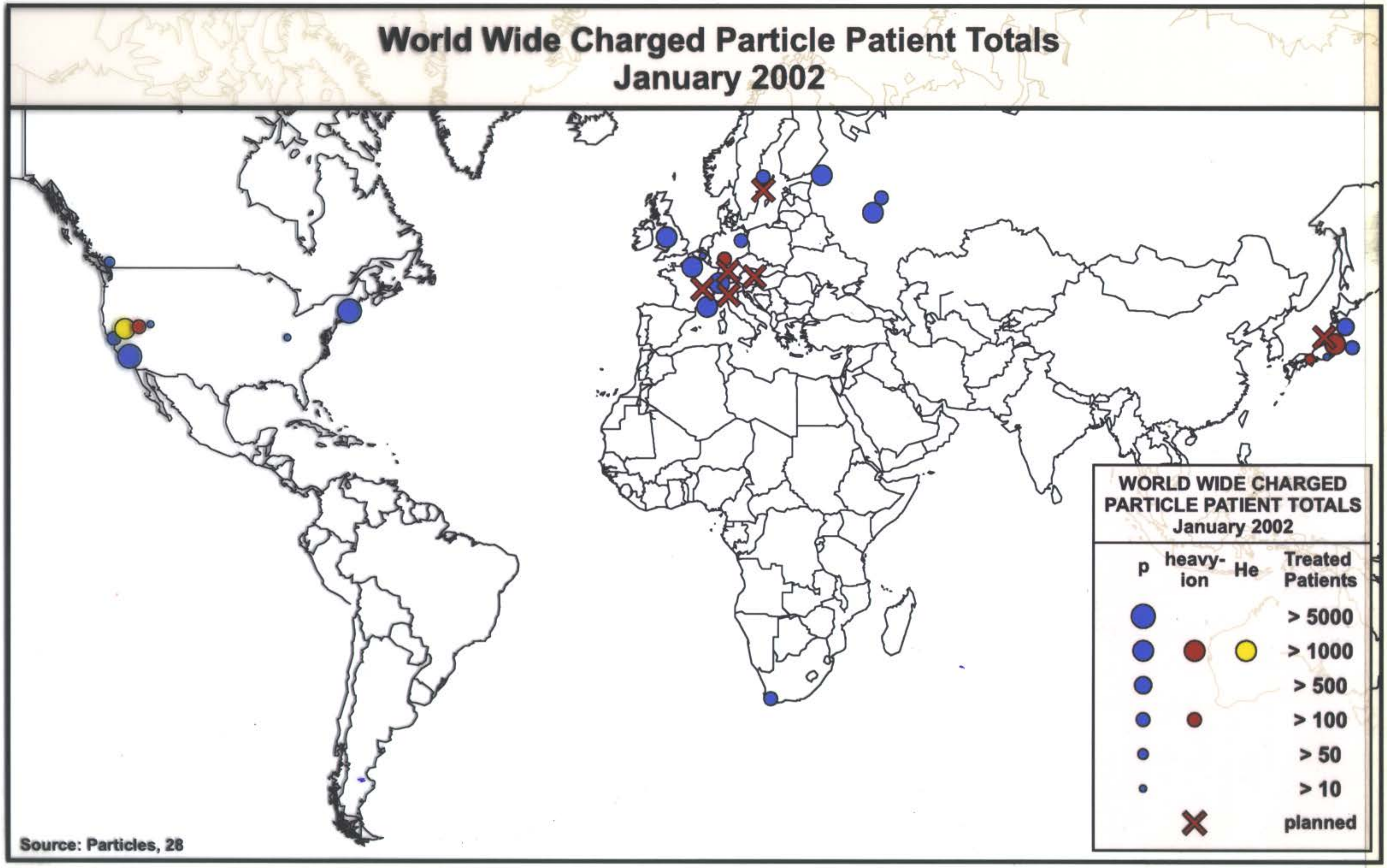
World Wide Charged Particle Patient Totals
January 2002
WORLD WIDE CHARGED PARTICLE PATIENT TOTALS
January 2002
p
heavy-ion
He
Treated Patients
> 5000
> 1000
> 500
> 100
> 50
> 10
planned
Source: Particles, 28

Advantages of heavy ion therapy

Inverse dose profile: higher target dose
lower dose to normal tissue

- Millimeter-precision treatment
- PET beam verification
- High biological effectiveness in the target
- Low biological effectiveness in the entrance channel
- Biological based treatment planning
- Little side effects
- Good tumor control rates 80-90%

Future

- Heavy ion center at Heidelberg
- Many projects over the world
- Treatment of moving organs
- Biologically optimized treatment